Thermodynamical, Structural and Clustering Properties of a Microemulsion Model

Munir S. Skaf[1] and George Stell

Chemistry Department
State University of New York at Stony Brook
Stony Brook, NY 11794

SUNY CEAS Report #621, March 1992

Abstract

A lattice version of the microemulsion model introduced by A. Ciach, J. Høye and G. Stell [*J. Chem. Phys.* **90**, 1214 (1989)] (CHS) is studied within a mean-field approximation. In the absence of (orientational) surfactant-surfactant interactions, an exact integration of the amphiphiles' orientational degrees of freedom in the CHS model yields an effective spin-one Hamiltonian with multi-body, temperature dependent interactions between particles, closely resembling the model introduced by M. Schick and W. H. Shih, [*Phys. Rev. Lett.* **59**, 1205 (1987)] and subsequently studied by Gompper and Schick. The phase diagram for the CHS effective Hamiltonian on a two-dimensional lattice is calculated at a mean-field level. Comparisons with selected results from Schick's model are then discussed. The calculated structure functions are in qualitative agreement with experimental results, showing a structural evolution from water-in-oil, to bicontinuous, to oil-in-water microemulsions as the water to oil concentration ratio is varied. The symmetric ($\rho^W = \rho^O$) subspace of the disordered phase of both models is then investigated using a percolation theory previously introduced by the authors. In both models the bicontinuous microemulsion phase is identified as a region of the phase diagram where the three molecular species are simultaneously percolating. Finally, the percolation threshold lines are investigated, for both models, as functions of their energy couplings. We find, again, similar behavior for the CHS effective Hamiltonian and Schick Hamiltonian. However, the thresholds are found to be more sensitive to the amphiphilic strength of the surfactant in the former.

---

[1]Present address: Chemistry Department, Colorado State University, Fort Collins, CO 80523

1 Introduction

From the standpoint of microscopic theories of microemulsions one would like to understand both the phase diagram, which is very rich in structure, and the underlying microscopic structural changes that can occur within the disordered phase. The later are particularly important in connection with the formation of the microemulsion phase itself. It seems that many of the unique properties of these systems, like the inability of the microemulsion to wet the water-oil interface, the extremely low surface-tension between water and oil, and also the very distinction between an ordinary disordered fluid and the microemulsion phase, stems from its structural properties [1,2,3]. Both the phase diagram and the structure functions for the disordered phase have received considerable attention in the literature for the last few years ([3,4,5,6,8,12,9,10,11]). Although a good qualitative picture has emerged from these studies, it is safe to say that the thermodynamic phase behavior of microemulsions is still far from completely understood on the basis of a single Hamiltonian model. Not surprisingly, different models are able to explain some properties better than others. For instance, it is known that the disordered phase coexists with water- and oil-rich phases and that many spatially modulated phases are present at higher concentrations of surfactant [16,17,18,19]. The model proposed by Widom and collaborators [4] captures this later feature but fails to produce the former, while in the model proposed by Schick[1,20] the trend is reversed. There is first-order transition between disordered and water/oil-rich phases, but among the lyotropic phases only the lamellar phase

seems to be present. A good comparison between some of the available results of different lattice models can be found in reference [21]. However, the most successful models are still not fully investigated, and much remain to be done before a comprehensive comparision among them can be made. One anticipates that such a comparision will help us to understand better the actual microphysics of surfactant mixtures, and prove useful in the pursuit of a more refined theory for microemulsions. In this work we shall explore a connection between two apparently very different lattice models, namely, the model introduced earlier by Ciach, Høye and Stell[8,7] (CHS) and a model due to Schick and collaborators[1,3,20]. This is accomplished by integrating the surfactant orientational degrees of freedom in the partition function of the CHS model, which leads to an effective Hamiltonian with interactions similar to those present in the Schick model. Using the effective Hamiltonian formulation we study the phase diagram and also the structure functions for the disordered phase of the model in two dimensions within a local mean-field approximation. From the knowledge of the structure functions we then investigate the bicontinuous phases of both, the CHS effective Hamiltonian model and the Schick model, from the perspective of a percolation theory recently proposed[22] to study site-correlated percolation problems in Hamiltonian models of microemulsions. For both models we find that, within a mean-field-like approximation, the bicontinuous microemulsion phase contains a part of the phase diagram where the three molecular species are simultaneously percolating. The threshold lines are then investigated as functions of the coupling energies of both models.

The remaider of the paper is organized as follows. In the next section, following Ciach [9], we recast the CHS model into more convenient form. In section 3 we present a description of the local mean-field approximation and calculate the instability of the disordered phase induced by modulated fluctuations of the order parameters. In section 4 we perform an exact integration of the surfactant orientations in the partition function of the CHS model to obtain an effective Hamiltonian which contains temperature-dependent many-body interactions involving only structureless occupation variables. Similarities with Schick's model are then discussed. A local mean-field theory is used again in section 5 to study the phase diagram of the effective Hamiltonian on a two dimensional lattice with emphasis on transitions to the disordered phase. In section 6 we study the behavior of the scattering functions for the disordered phase and some qualitative comparisons are made with experimental results. Finally, in section 7 we briefly present our approach to percolation in these systems and apply it to investigate some clustering properties of the bicontinuous phases of two microemulsion models.

2 CHS Lattice Model

In the lattice version of the CHS model introduced in Refs. [8,7] every site of a lattice, taken to be hypercubical for simplicity, is occupied by a single particle of some kind. Interactions are considered only between pairs of particles which are on nearest-neighbor sites. The Hamiltonian of the mixture can be written in terms of multicomponent lattice gas variables, which in a

general form is given by

$$\mathcal{H} = -\sum_{i \leq j} \sum_{<\mathbf{r},\mathbf{r}'>} \epsilon_{ij}(\mathbf{r}' - \mathbf{r})\, n_j(\mathbf{r})\, n_i(\mathbf{r}') - \sum_j \sum_{\mathbf{r}} \mu_j\, n_j(\mathbf{r}) \; . \qquad (1)$$

The variables $n_j(\mathbf{r})$ assume values 0 or 1 depending on whether the site $\mathbf{r}$ is occupied by a particle of species j or not. (The surfactant molecules with different orientations can be viewed as different species in the mixture [7].) The sums in i and j are over the $2+2d$ "components" of the mixture ($i = 1, 2$ refers to water and oil respectively, while $i \geq 3$ refers to the amphiphile particles with their $2d$ possible orientations. For obvious reasons $\mu_i = \mu_j \equiv \mu_S$ for all $i, j \geq 3$. (The terms amphiphile and surfactant are used interchangeably throughout this work.) One of the essential characteristics of the model is the fact that the amphiphile particles have selective ends, i.e. the interaction strength between, say, water and amphiphile is changed if the water molecule is replaced by an oil molecule or if the relative orientation of the amphiphile is reversed. This is accomplished by an asymmetry in the interaction couplings ϵ_{ij} with respect to spatial inversion or with the interchange of the labels i and j when either i or $j \geq 3$ as discussed in [7]. By introducing spin-1 variables

$$S(\mathbf{r}) = n_1(\mathbf{r}) - n_2(\mathbf{r}) \; ; \; S_j(\mathbf{r}) = n_{2j+2}(\mathbf{r}) - n_{2j+1}(\mathbf{r}) \; ; \; j = 1, 2, ..., d \qquad (2)$$

the Hamiltonian can be conveniently [9] written as

$$\mathcal{H} = \mathcal{H}_o + \mathcal{H}_1 + \mathcal{H}_2 \qquad (3)$$

where $\mathcal{H}_o$ is of the form of the Blume, Emery and Griffiths [23] (BEG) model

$$\mathcal{H}_o = -\sum_{<\mathbf{r},\mathbf{r}'>} [J\, S(\mathbf{r})S(\mathbf{r}') + K\, S^2(\mathbf{r})S^2(\mathbf{r}')] - H \sum_{\mathbf{r}} S(\mathbf{r}) + \Delta \sum_{\mathbf{r}} S^2(\mathbf{r}) . \quad (4)$$

The couplings J and K, as well as the fields H and Δ, are trivially related to the particle-particle couplings and chemical potentials through the relations

$$J = (\epsilon_{11} + \epsilon_{22} + 2\epsilon_{12})/8 \;\; ; \;\; K = (\epsilon_{11} + \epsilon_{22} - 2\epsilon_{12})/8$$
$$H = (\mu_1 - \mu_2)/2 \;\; ; \;\; \Delta = \mu_s - (\mu_1 + \mu_2)/2 \; . \tag{5}$$

The second term in (3) represents the interactions of the surfactant with oil and water, which can be written as

$$\mathcal{H}_1 = -c \sum_{\mathbf{r}} \sum_{j=1}^{d} S(\mathbf{r}) \, [S_j(\mathbf{r} + \mathbf{e}_j) - S_j(\mathbf{r} - \mathbf{e}_j)] \; , \tag{6}$$

where we have assumed the surfactant interacts equally strongly with water and oil. The third term in (3) is an interaction between amphiphiles which favors the molecules to be parallel to each other. Such an interaction can be written as

$$\mathcal{H}_2 = -\frac{1}{2} g \sum_{\mathbf{r}} \sum_{j=1}^{d} \sum_{\delta_\perp} S_j(\mathbf{r}) \, S_j(\mathbf{r} + \delta_\perp) \; , \tag{7}$$

where $\delta_\perp$ corresponds to the $2(d-1)$ nearest-neighbor sites in the directions perpendicular to the direction j. The spin variables are subject to the constraint $S^2(\mathbf{r}) + \sum_{j=1}^{d} S_j^2(\mathbf{r}) = 1$ which reflects the fact that there are no empty sites on the lattice.

Several studies on this model or variations thereoff, have been published in the last few years [7,8,9,10,11]. Very recently Matsen and Sullivan [13] studied a one-dimensional version of the CHS model with results similar to those of reference [11]. They have also studied interfacial properties of a slightly modified version of the CHS Hamiltonian within the mean-field and Bethe

approximations [14]. Also recently, Laradji *et.al.* [15] have performed large-scale Monte Carlo simulations of the CHS model on square lattices and also presented mean-field results which are similar to those reported in reference [9]. The Hamiltonians used in references [13,14,15] may be better recognized as the CHS model (with slight variations in the case of reference [14]) when the CHS Hamiltonian is written in the form of equation (25) (see section 4).

3 Boundary of Instability of the Disordered Phase

In order to study phase coexistence and instability of the system we introduce a set of local order-parameter fields defined by

$$\begin{aligned} \eta(\mathbf{r}) &= < S(\mathbf{r}) > \;\; ; \;\; \rho(\mathbf{r}) = < S^2(\mathbf{r}) > \\ M_j(\mathbf{r}) &= < S_j(\mathbf{r}) > \;\; ; \;\; Q_j(\mathbf{r}) = < S_j^2(\mathbf{r}) > \;\; . \end{aligned} \tag{8}$$

Here η measures the local water and oil concentration difference, $\rho^S = 1 - \rho$ measures the surfactant concentration (irrespective of orientation), Q_j gives the concentration of surfactant with principal direction j, while M_j specifies its orientation along this principal direction. The simplest theory is a mean-field one, where the free energy functional is given by a standard expression

$$\begin{aligned} F^{MF} \;=\; & -\sum_{<\mathbf{r},\mathbf{r}'>} [J\,\eta(\mathbf{r})\,\eta(\mathbf{r}') + K\,\rho(\mathbf{r})\,\rho(r')] - \sum_{\mathbf{r}} [H\,\eta(\mathbf{r}) - \Delta\,\rho(\mathbf{r})] \\ & -c \sum_{\mathbf{r}} \sum_{j=1}^{d} \eta(\mathbf{r}) \left[M_j(\mathbf{r}+\mathbf{e}_j) - M_j(\mathbf{r}-\mathbf{e}_j) \right] \\ & -\frac{g}{2} \sum_{\mathbf{r}} \sum_{j=1}^{d} \sum_{\delta_\perp} M_j(\mathbf{r})\, M_j(\mathbf{r}+\delta_\perp) \end{aligned} \tag{9}$$

$$+T\sum_{\mathbf{r}}\Big[\frac{\rho(\mathbf{r})+\eta(\mathbf{r})}{2}\ln\frac{\rho(\mathbf{r})+\eta(\mathbf{r})}{2}+\frac{\rho(\mathbf{r})-\eta(\mathbf{r})}{2}\ln\frac{\rho(\mathbf{r})-\eta(\mathbf{r})}{2}\Big]$$
$$+T\sum_{\mathbf{r}}\sum_{j}\Big[\frac{Q_j+M_j}{2}\ln\frac{Q_j+M_j}{2}+\frac{Q_j-M_j}{2}\ln\frac{Q_j-M_j}{2}\Big].$$

In order to study the phase diagram this functional must be minimized with respect to the order parameters under the constraint

$$\Psi=\sum_{j=1}^{d}Q_j(\mathbf{r})+\rho(\mathbf{r})-1=0\,. \tag{10}$$

This procedure yields then self-consistent equations for the order parameter fields whose solutions are used to calculate the value of the free energy. These equations, which are easily obtained by means of a local Lagrange multiplier, are given by

$$\eta(\mathbf{r}) = \rho(\mathbf{r})\tanh a(\mathbf{r}) \tag{11}$$
$$\rho(\mathbf{r}) = [1+e^{-b(\mathbf{r})}\mathrm{sech}\,a(\mathbf{r})\sum_{j=1}^{d}\cosh\,b_j(\mathbf{r})]^{-1} \tag{12}$$
$$M_j(\mathbf{r}) = Q_j(\mathbf{r})\tanh\,b_j(\mathbf{r}) \tag{13}$$
$$Q_j(\mathbf{r}) = [1-\rho(\mathbf{r})]\cosh\,b_j(\mathbf{r})[\sum_{j=1}^{d}\cosh b_j(\mathbf{r})]^{-1}\,, \tag{14}$$

where

$$\begin{aligned}
a(\mathbf{r}) &= \beta J\sum_{j=1}^{d}\big[\eta(\mathbf{r}+\mathbf{e}_j)+\eta(\mathbf{r}-\mathbf{e}_j)\big] \\
&\quad +c\sum_{j=1}^{d}[M_j(\mathbf{r}+\mathbf{e}_j)-M_j(\mathbf{r}-\mathbf{e}_j)]+\beta H \\
b(\mathbf{r}) &= \beta K\sum_{j=1}^{d}\big[\rho(\mathbf{r}+\mathbf{e}_j)+\rho(\mathbf{r}-\mathbf{e}_j)\big]-\beta\Delta \qquad (15)\\
b_j(\mathbf{r}) &= \beta c\,[\eta(\mathbf{r}-\mathbf{e}_j)-\eta(\mathbf{r}+\mathbf{e}_j)]+\beta g\sum_{\delta_\perp}[M_j(\mathbf{r}+\delta_\perp)+M_j(\mathbf{r}-\delta_\perp)].
\end{aligned}$$

There will be in general many solutions of these equations representing different candidates for the density profiles. At a given temperature and chemical potentials the stable phase corresponds to that solution for which the free energy is a global minimum. When two or more solutions of these equations have the same minimal value for the free energy, at fixed temperature and chemical potentials, the corresponding phases are said to coexist. To construct the entire phase diagram is a formidable task in view of the fact that many periodically ordered phases are presumably present. In section 5 we shall carry out part of such a program for a special case, once we have eliminated the orientational degrees of freedom and thus reducing the number of order parameter fields in the problem.

For uniform phases the problem becomes very simple. In this case we have $\eta(\mathbf{r}) = \eta$, $\rho(\mathbf{r}) = \rho$, $M_j(\mathbf{r}) = M$ and $Q_j(\mathbf{r}) = Q$. Minimization of the free energy leads to the equations

$$\begin{aligned} \beta H &= \frac{1}{2} \ln \frac{\rho+\eta}{\rho-\eta} - 2\,d\,\beta\,J\,\eta \\ \beta\Delta &= 2\,d\,\beta K\rho - \frac{1}{2}\ln\left(\rho^2-\eta^2\right) + \ln\frac{1-\rho}{d} - \ln\cosh\left[(d-1)\beta g M\right] \\ M &= \frac{1-\rho}{d}\tanh\left[(d-1)\beta g M\right] \ . \end{aligned} \tag{16}$$

The disordered phase in the symmetric case $H = 0$, where water and oil are present in equal amounts is characterized by the solution $\eta_o = M_o = 0$ with ρ_o given by the solution of the equation (16) for a given temperature and surfactant chemical potential Δ. Notice that at this level of approximation the interaction between amphiphile and ordinary particles gets completely washed away when considering spatially uniform phases. This can be seen,

for instance, from the expression for the free energy functional (equation 9). This means that the tricritical temperature, below which the disordered phase coexists with water- and oil-rich phases, is essentially the one given by the Blume, Emery and Griffiths [23] (BEG) model. We shall see shortly that this temperature is much too low and that a transition between the disordered phase and a lyotropic modulated phase will preclude the existence of such a tricritical temperature in this mean-field treatment.

In order to determine the boundary of instability of the disordered phase it is convenient to work in Fourier space considering small fluctuations around the uniform solutions of the order parameters, keeping only terms through second-order in a Landau-Ginzburg expansion of the free-energy functional. The Fourier expansions of the order parameters are written as

$$\chi(\mathbf{r}) = \chi_o + \sum_{\mathbf{k}\neq 0} \chi(\mathbf{k})\, e^{i\mathbf{k}.\mathbf{r}} \ , \tag{17}$$

where χ stands for η , ρ , M_j or Q_j. In the symmetric case we have $\eta_o = M_o = 0$ and $Q_o = (1-\rho_o)/d$. Expanding (9) up to second order in the Fourier amplitudes, we obtain

$$F^{MF} = F_o^{MF} + \sum_{\mathbf{k}} f_{\mathbf{k}} \ , \tag{18}$$

with

$$\begin{aligned} f_{\mathbf{k}} \ = \ & \alpha_{\mathbf{k}}\, \eta(-\mathbf{k})\, \eta(\mathbf{k}) + \beta_{\mathbf{k}}\, \rho(-\mathbf{k})\, \rho(\mathbf{k}) \\ & + \sum_{j=1}^{d} \Big[\gamma_{\mathbf{k}}^{j} \Big(\eta(\mathbf{k})\, M_j(-\mathbf{k}) - \eta(-\mathbf{k})\, M_j(\mathbf{k}) \Big) \\ & + \frac{1}{2Q_o} Q_j(-\mathbf{k})\, Q_j(\mathbf{k}) + \Omega_{\mathbf{k}}^{j}\, M_j(-\mathbf{k})\, M_j(\mathbf{k}) \Big] \ , \end{aligned} \tag{19}$$

where

$$\alpha_{\mathbf{k}} = \frac{T}{2\rho_o} - J\lambda(\mathbf{k}) \;\; ; \;\; \beta_{\mathbf{k}} = \frac{T}{2\rho_o} - K\lambda(\mathbf{k})$$
$$\Omega^j_{\mathbf{k}} = \frac{T\,d}{2(1-\rho_o)} - g\,\lambda^j_{\perp}(\mathbf{k}) \;\; ; \;\; \gamma^j_{\mathbf{k}} = i\,c\,\sin(k_j) \tag{20}$$

and

$$\lambda(\mathbf{k}) \;=\; \sum_{j=1}^{d} \cos(k_j) \;\; ; \;\; \lambda^j_{\perp}(\mathbf{k}) = \sum_{i\neq j} \cos(k_i) \quad . \tag{21}$$

The quadratic form $f_{\mathbf{k}}$ can be cast in a matrix representation and diagonalized in a standard way. In three dimensions its determinant is given by

$$\det(T,\Delta,\mathbf{k}) \;=\; \alpha_{\mathbf{k}}\,\Omega^1_{\mathbf{k}}\,\Omega^2_{\mathbf{k}}\,\Omega^3_{\mathbf{k}} + (\gamma^1_{\mathbf{k}})^2\,\Omega^2_{\mathbf{k}}\,\Omega^3_{\mathbf{k}} + (\gamma^2_{\mathbf{k}})^2\,\Omega^1_{\mathbf{k}}\,\Omega^3_{\mathbf{k}} + (\gamma^3_{\mathbf{k}})^2\,\Omega^1_{\mathbf{k}}\,\Omega^2_{\mathbf{k}} \;, \tag{22}$$

where it is understood that ρ_o is the solution of the equation $\beta\Delta = 6\beta K\rho_o + \ln(Q_o/\rho_o)$, which is obtained from equation (16). A second-order phase transition from the disordered phase into an ordered state of wavevector $\mathbf{k}$ occurs when

$$\det(T,\Delta,\mathbf{k}) \;=\; 0 \quad . \tag{23}$$

At a given surfactant chemical potential Δ the wavevector $\mathbf{k} = \mathbf{k}_c$ characterizing the periodically ordered state is the one for which the solution of the equation above has the highest T. This condition then generates the locus of critical points of the disordered phase in the (T,Δ)-plane.

In Figure 1 we show this critical line for some representative values of the coupling constants for the symmetric case $H = 0$. At smaller values of the surfactant concentration, i.e. to the left of the point $k_c = 0$ where

$\rho^S = 0.129$, the disordered phase undergoes a continuous phase transition into uniform water-rich and oil-rich phases. At higher surfactant concentrations the system prefers to organize itself into a liquid-crystalline phase of wavevector $k_c \neq 0$. We have found that the highest temperatures in the solution of (23) occur along the direction (1,1,1). (The system is not rotationally invariant because of the lattice.) In Figure 2 we show k_c versus surfactant concentration along the critical line of Figure 1. If there were a tricritical point in this approximation it would be located at $T_{tc}/J = 3.6$ and $\rho^S_{tc} = 0.4$. Below this temperature the line of critical points between disordered and water-rich/oil-rich phases would merge into a triple line along which these phases would coexist. The point to notice here is that the system would prefer to order into some modulated phase much before this temperature can be reached from above, thus precluding three-phase coexistence between the disordered and the uniform water/oil-rich phases in disagreement with experiments [16,17]. We point out however, that almost surely this is not attributable to a fault in the model, but it is a consequence of the mean-field approximation which averages out the anti-symmetric pair-interactions between the surfactant and the ordinary particles for uniform phases. In section 5 we shall see how this can be easily remedied.

So far we have found the line of second-order transitions separating the disordered fluid from other phases. This line may not reflect the actual boundary of existence of the disordered phase of the model for *all* values of surfactant chemical potential since a first-order transition into a modulated phase could take place at temperatures higher than the ones given by line of continuous

transitions we have determined. A more complete scenario including first-order transitions between phases will be given in section 5. First let us derive an effective Hamiltonian for the CHS model where the number of order parameter fields gets reduced.

4 Summation of the Surfactant Orientations

In the spin-1 model developed by Schick and collaborators the amphiphilic nature of the surfactant particles is represented by a three-body potential which favors the surfactant molecules sitting between the water and oil molecules. It has been suggested [3] that this interaction should not be thought of as a real three-particle molecular interaction, but rather that it can be thought of as resulting from an angular integration of a more fundamental, orientation dependent, interaction between surfactant and nonsurfactant particles. In fact, it has been shown [24,25] that an integration over the directional degrees of freedom in binary mixtures of water and surfactant leads to a Hamiltonian with temperature-dependent coupling energies between clusters of three and more (structureless) particles. It is, therefore, natural to adopt here similar procedure for the CHS ternary system.

First we notice that the oriented surfactant occupancy variables S_j can be written as

$$S_j(\mathbf{r}) = [1 - S^2(\mathbf{r})]\,\sigma_j(\mathbf{r}) \tag{24}$$

where $[1 - S^2(\mathbf{r})]$ determines whether the site $\mathbf{r}$ is occupied by an amphiphile molecule or not, while the variable $\sigma_j(\mathbf{r}) = \pm 1$ specifies its orientation along

the j^{th} direction in case the site is occupied by an amphiphile. The equations (6) and (7) become

$$\mathcal{H}_1 = -c\sum_{\mathbf{r}}\sum_{j=1}^{d} S(\mathbf{r})\Big([1-S^2(\mathbf{r}+\mathbf{e}_j)]\,\sigma_j(\mathbf{r}+\mathbf{e}_j) - [1-S^2(\mathbf{r}-\mathbf{e}_j)]\,\sigma_j(\mathbf{r}-\mathbf{e}_j)\Big)$$

$$\mathcal{H}_2 = \frac{1}{2}\,g\sum_{\mathbf{r}}\sum_{j=1}^{d}[1-S^2(\mathbf{r})]\,[1-S^2(\mathbf{r}-\mathbf{e}_j)]\,\sigma_j(\mathbf{r})\,\sigma_j(\mathbf{r}-\mathbf{e}_j)\quad . \tag{25}$$

The partition function is given by

$$\mathcal{Z} = \sum_{\{S\}} e^{-\beta\mathcal{H}_o}\sum_{\{\sigma\}} e^{-\beta(\mathcal{H}_1+\mathcal{H}_2)}\ . \tag{26}$$

When the interaction between oriented amphiphiles is neglected the sum over the variables σ can be carried out at once since the σ_j's are not coupled to one another in $\mathcal{H}_1$. One is left with a partition function of the form

$$\mathcal{Z} = \sum_{\{S\}} e^{-\beta(\mathcal{H}_o+\mathcal{H}_{\text{eff}})}\ , \tag{27}$$

where the effective Hamiltonian $\mathcal{H}_{\text{eff}}$, which depends solely on the structureless occupational variables S, is given by

$$\mathcal{H}_{\text{eff}} = -\sum_{\mathbf{r}}[1-S^2(\mathbf{r})]\,\ln\sum_{j=1}^{d} 2\cosh\Big(\beta c\,[S(\mathbf{r}+\mathbf{e}_j)-S(\mathbf{r}-\mathbf{e}_j)]\Big)\ . \tag{28}$$

The logarithmic function above can be exactly written as a polynomial in the variables S for various lattices since $S^3 = S$ (recall that for every site$S(\mathbf{r})$ can assume only the values $0, \pm 1$.) For a one dimensional chain this polynomial is easily obtained and $\mathcal{H}_{\text{eff}}$ is simply given by

$$\mathcal{H}_{\text{eff}}^{d=1} = \sum_{x}[1-S^2(x)]\Big[J_1\,S(x+1)\,S(x-1) + J_2\,S^2(x+1) + J_3\,S^2(x+1)\,S^2(x-1)\Big]\ . \tag{29}$$

where the temperature dependent couplings are

$$J_1 = -\frac{1}{2}\ln(2\cosh 2\beta c)\ ;\ J_2 = \ln(2\cosh \beta c)\ ;\ J_3 = -J_1 - J_2 \qquad (30)$$

This Hamiltonian presents a striking similarity with Schick's. The term in J_1 reflects the amphiphilic nature of the surfactant molecules by favoring configurations where they sit between water and oil particles. The second term merely renormalizes the coupling K and the surfactant chemical potential in the Hamiltonian $\mathcal{H}_o$. It is worth noticing that the terms in J_2 and J_3 represent interactions between structureless amphiphiles which are a by-product of the interactions between water and oil with an oriented surfactant molecule. The last two terms in (29) are not present in Schick's model. Nevertheless, we have found that the topology of the one dimensional phase diagram remains unaltered within mean-field theory. Similar polynomial expansions for (28) are obtained in two or three dimensions. For a two-dimensional square lattice such a polynomial is derived in the Appendix A. There we find that, besides terms like the ones above, many other multi-particle interactions appear. The phase diagram in this case is somewhat different from the one given by the Schick's model as we shall show by applying the mean-field theory of section 3 to the effective Hamiltonian in the upcoming section.

We close this section with a comment on a similar relationship between earlier versions of the Alexander [26] and the Widom-Wheeler [27] models. In the later the sites of a hypercubical lattice are filled with a spin-1/2 variable assuming values $\sigma = \pm 1$. Every nearest-neighbor pair of $+1$ spins represents a water molecule, every nearest-neighbor pair of -1 spins represents an oil

molecule and every pair of opposite spins represents an amphiphile. The particles are thought of as located on the bonds between sites. In this way water and oil are always separated by a correctly oriented amphiphile. The Alexander model is also a spin-1/2 model, but one in which the water and oil molecules are represented by the two spin states on each site. An additional variable $p = 0, 1$ is placed on the bonds between sites indicating whether a surfactant molecule is present or not. In this model, water and oil are not necessarily separated by an amphiphile, but their separation depends on temperature and on the strength of the bonds governed by the variables p. When no interaction between these bonds is considered one can integrate out the variables p in the partition function obtaining an effective spin-1/2 Hamiltonian very similar to that of the Widom-Wheeler model.

5 Mean-Field Results for $\mathcal{H}_{\text{eff}}$

The integration of the surfactant orientations in the CHS model left us with a very long Hamiltonian when written as a polynomial (Appendix A). Nevertheless, its treatment via mean-field theory is much easier to handle since now we have only two order-parameter fields, namely, $\eta(\mathbf{r})$ and $p(\mathbf{r})$. Obviously, both the original CHS and the $\mathcal{H}_{\text{eff}}$ formulations yield the very same thermodynamic and structural properties if these could be obtained in an exact way for any dimension. However, this is not the case when using approximation methods. For instance, in section 3 we saw that the mean-field approximation averages out the effects of the surfactant interactions with wa-

ter and oil in the original CHS formulation when considering uniform phases. We shall see here that this is not so when a mean-field theory is applied to the model after the summation of the amphiphile orientation is done in the partition function, with a subsequent polynomial expression for the resulting effective Hamiltonian. We have found that as long as one is not seeking properties which depend directly on the surfactant orientations, it is more convenient to work with the effective Hamiltonian where the orientations have been implicitly accounted for. The results we report here are for a two-dimensional square lattice. In view of the ground-state properties of the model [7] it is evident that the phase diagram for a three-dimensional system is much richer in structure due to the presence of 3-d modulated phases like the cubic phase. However, as far as mean-field theory is concerned we expect our calculations to exhibit the characteristic features of the full model for those parts of the phase diagram where three-dimensional structures are not present. The treatment we shall give here and in the next section, follows very closely the one of reference [3] due to the similarity of both Hamiltonians. We shall concentrate on the symmetric subspace in which $H = 0$ and where the surfactant interacts equally strongly with water and oil. In this case the mixture is said to be balanced, i.e. water and oil are present in equal amounts in the system. Therefore there are only two external parameters to be varied, namely, the temperature and the surfactant chemical potential. The symmetric model is expected to describe real mixtures containing only non-ionic surfactants where the system balances at water to oil concentration ratios very close to one. For ionic surfactants one must take into account the fact that there is asymme-

try in the interactions between the surfactant and the other two components [6,16]. The effective Hamiltonian in this case is somewhat different from the one we have derived here.

The free energy functional is given by

$$F^{MF} = \overline{\mathcal{H}} + T \sum_{\mathbf{r}} [\frac{\rho+\eta}{2} \ln \frac{\rho+\eta}{2} + \frac{\rho-\eta}{2} \ln \frac{\rho-\eta}{2} + (1-\rho) \ln (1-\rho)], \quad (31)$$

where $\overline{\mathcal{H}} = \overline{\mathcal{H}_o} + \overline{\mathcal{H}}_{\rm eff}$. Here $\overline{\mathcal{H}_o}$ denotes the BEG energy given by

$$\overline{\mathcal{H}_o} = - \sum_{<\mathbf{r},\mathbf{r}'>} [J\,\eta(\mathbf{r})\,\eta(\mathbf{r}') + K\,\rho(\mathbf{r})\,\rho(r')] - \sum_{\mathbf{r}} [H\,\eta(\mathbf{r}) - \Delta\,\rho(\mathbf{r})] \ . \quad (32)$$

The energy functional $\overline{\mathcal{H}}_{\rm eff}$ is obtained by replacing the site occupation variables $S(\mathbf{r})$ and $S^2(\mathbf{r})$ in the effective Hamiltonian derived in the Appendix A by their respective average values. The result is given by

$$\overline{\mathcal{H}}_{\rm eff} = - \sum_{\mathbf{r}} (1-\rho)\, h(\mathbf{r}) \quad (33)$$

with

$$\begin{aligned} h(\mathbf{r}) \ = \ & \sum_{j=1}^{2} \Big[J_1\,\eta(\mathbf{r}-\mathbf{e}_j)\,\eta(\mathbf{r}+\mathbf{e}_j) + J_2\,\rho(\mathbf{r}+\mathbf{e}_j) + J_3\,\rho(\mathbf{r}-\mathbf{e}_j)\,\rho(\mathbf{r}+\mathbf{e}_j) \Big] \\ & + J_4\,\Delta^x\rho\,\Delta^y\rho + J_5(\Pi^x\eta\,\Delta^y\rho + \Pi^y\eta\,\Delta^x\rho) + J_6(\,\Pi^x\rho\,\Delta^y\rho + \Pi^y\rho\,\Delta^x\rho) \\ & + J_7(\Pi^x\eta\,\Pi^y\rho + \Pi^y\eta\,\Pi^x\rho) + J_8\,\Pi^x\eta\,\Pi^y\eta + J_9\,\Pi^x\rho\,\Pi^y\rho \ . \end{aligned} \quad (34)$$

Throughout these expressions it is understood that $\eta = \eta(\mathbf{r})$ and $\rho = \rho(\mathbf{r})$. Also $\Pi^j f(\mathbf{r}) = f(\mathbf{r}+\mathbf{e}_j) f(\mathbf{r}-\mathbf{e}_j)$ and $\Delta^j f(\mathbf{r}) = f(\mathbf{r}+\mathbf{e}_j) + f(\mathbf{r}-\mathbf{e}_j)$ for $j = x, y$. The temperature dependent couplings are given in Appendix A. Minimization of the free energy functional (31) leads to equations for the order parameters fields $\eta(\mathbf{r})$ and $\rho(\mathbf{r})$ which are very similar to the ones given in section 3.

At high temperatures the stable state is a uniform disordered phase characterized by $\eta(\mathbf{r}) = \eta_o = 0$ and $\rho(\mathbf{r}) = \rho_o$ where these values are obtained from the uniform self-consistent equations. As we lower the temperature at low surfactant concentrations we find no spatially modulated phases, so that the system separates into uniform water-rich and oil-rich phases characterized by $\eta \neq 0$. In a magnetic language the disordered phase is paramagnetic while the water/oil-rich phase is ferromagnetic. In order to study these transitions the free energy for uniform η and ρ is expanded around the disordered state à la Ginzburg-Landau [3,23,28]. The expansion has the form

$$\beta F^{MF} = \beta F_o + A_2(T,\Delta)\eta^2 + A_4(T,\Delta)\eta^4 + \ldots \quad . \tag{35}$$

The coefficient A_2 is given by

$$A_2(T,\Delta) = \frac{T}{2\rho_o} - 2\,\beta\,J - (1-\rho_o)\,(\,2\,J_1 + 2\,\rho_o\,J_5 + \rho_o^2\,J_7\,) \tag{36}$$

where for given T and Δ, ρ_o is the solution of

$$\begin{aligned} \Delta \;\; = \;\; & 4\,K\,\rho + 2\,J_2(1-2\rho) + 2(J_3 + 2\,J_4)\,\rho\,(2-3\rho) \\ & +4\,J_6\,\rho^2\,(3-4\rho) + J_9\,\rho^3\,(4-5\rho) + T\;\ln\frac{2(1-\rho)}{\rho} \quad . \end{aligned} \tag{37}$$

In this way we have minimized the free energy with respect to ρ, but not with respect to η. By standard minimization with respect to η we find that the equation $A_2(T,\Delta) = 0$ defines a line of critical points, along which the transition between disordered and water/oil-rich phases is of the second order. This line terminates at a tricritical point whose position is given by the solution of $A_4(T,\Delta) = 0$. For temperatures below the tricritical point the transition is of

the first order, therefore there exists three-phase coexistence between the disordered phase and the water-rich and oil-rich phases. The line of three-phase coexistence, commonly referred to as the triple line, is most easily found by determining the Δ, as a function of temperature, for which the free energies of the disordered phase ($\eta = 0$) and the water/oil-rich phases ($\eta \neq 0$) are equal to each other. (Recall that in the symmetric model both water-rich and oil-rich phases have the same free energy.) For larger values of Δ,which means higher surfactant concentrations, the system develops spatially modulated phases. The strategy in this case is as follows. First we use the Landau expansion for the free energy in Fourier space to determine continuous transitions between the disordered and modulated phases as discussed in section 3 (this expansion is found in the next section where we discuss the scattering functions). Next we write down the free-energy functional (31) along with the self-consistent equations for many different modulated phases and look for lines of coexistence with the disordered phase. At any given Δ the modulated phase which yields the highest transition temperature to the disordered state is the one that prevails. Thus, we are able to determine which modulated phase is in contact with the disordered phase in the phase diagram, as well as the nature of the transition. Because the particles are confined to a lattice there will also exist first order transitions between modulated phases of different periodicities. In real systems no such transitions take place, as the period of a certain modulated phase varies continuously with changes in the relative amount of the components of the mixture. This is not to be confused, however, with first-order transitions between modulated phases of different *dimensionality*.

These do occur in real systems, as well as in our model calculations.

A typical phase diagram in the (T, Δ)-plane is shown in Figure 3 for the symmetric model with $c/J = 6.0, K/J = 3.0$ and $H = 0$. First-order and second-order phase transitions separating the disordered from other phases are shown by solid and dashed lines respectively. The dotted line shown in Figure 3 is not a line of thermal phase transitions and can be ignored for the moment. (We shall refer to it in the next section.) The general trend shows a disordered phase undergoing second-order or first-order transitions into water-rich and oil-rich coexisting phases for small values of Δ (low surfactant concentration).These two regimes are separated by a tricritical point denoted by a full dot. As the amount of surfactant is increased the disordered phase becomes destabilized by the presence of a modulated phase which appears to be lamellar. Along this line the critical wavevector k_c varies continuously in the interval $(0, \pi/2)$ indicating the presence of modulated phases which may have very long periods. As the surfactant chemical potential is increased still further, the disordered phase coexists with a 2-d modulated block-phase of period four. The point where the solid line intercepts the dashed line on the right upper corner of Figure 3 is *not* a tricritical point. Below the disordered phase, at lower temperatures, there is three-phase coexistence between water-rich, oil-rich and lamellar phases. There is also coexistence between lamellar and 2-d block phases at higher values of Δ. However, we have made no attempts to determine the precise position of these lines. This is not the region of the phase diagram we are most interested in, and it is technically difficult to tune first-order transitions between modulated phases with non-constant periodic-

ities. Therefore, coexistence lines between lamellar and water/oil-rich, and between lamellar and 2-d block phases are shown by the solid-dashed lines in Figure 3 schematically, rather than with quantitative accuracy.

The general features of the phase diagram shown in this figure persist for weaker and stronger surfactants as well, with modulated phases occupying much of the phase diagram in the later case. Among the various sets of parameters we have done calculations for, we have not observed coexistence between the disordered and lamellar phases. The transition there seems to be always of the second order. (Such a coexistence of phases is actually expected theoretically [29] and have been found in the Monte Carlo simulation of the CHS model performed by Laradji *et. al.* [15].) Another point to notice is the fact that the range in surfactant chemical potential over which the disordered phase orders itself into a lamellar structure seems to be rather narrow, that is, a two dimensional ordered structure is thermodynamically more stable over larger portions of the phase diagram. At this point we are not able to answer if this scenario is peculiar of a two dimensional system or not. At any rate, a simple refinement on the model can be envisaged to probe the nature and relative range of existence of the lamellar-to-disordered transitions. It is easy to see that a second-nearest neighbor interaction between structureless amphiphiles of the form $-K_2 \sum_{<<\mathbf{r},\mathbf{r}'>>} [1 - S^2(\mathbf{r})][1 - S^2(\mathbf{r}')]$ tends to stabilize lamellar structures and hence could be used profitably for the purposes above.In this respect the mean-field phase diagram for the two-dimensional effective Hamiltonian is different from the one obtained in the Schick model. In this model the lamellar phase is very robust in the phase diagram given

the form of the interactions between surfactant and ordinary particles found in the model. However, we are not aware of the existence of other modulated phases in Schick's model.

6 Scattering Functions For The Disordered Phase

When microemulsion models were first proposed some years ago [7,20,30] it was initially thought that what the experimentalists called the microemulsion phase could be identified with the many lyotropic modulated phases encountered in the model calculations. It was soon realized [31], however, that the real microemulsion phase has an existence of its own, apart from the spatially ordered phases, which are also present in the experimental systems. Isotropy of the real microemulsion indicated that if the proposed models were to explain the existence of such a phase at all, it should be located within the disordered phase of these models. This view is also corroborated by the results of an earlier experimental work, which concluded that only a disordered fluid could explain the observed surfactant film scattering spectra [32]. What distinguishes then the microemulsion from an ordinarily disordered fluid ? The current view holds that the heart of the matter lies in the structural properties of the disordered phase [1,2]. Small angle x-ray and neutron diffraction experiments [32,33,34,35] show that the microemulsion exhibits a characteristic signature in its scattering functions. Unlike an ordinary disordered fluid, the microemulsion shows a maximum of the water-water scattering amplitude, which is located at non-zero values of the momentum transfer $\mathbf{k}$.

In this section we calculate the pertinent scattering functions in the disordered phase of the model in order to make some comparison with experimental results. In the spirit of section 3 we expand the free-energy functional (31) through second order in the Fourier components. However, we shall not restrict ourselves here to equal concentrations of water and oil, i.e. η_o is not necessarily zero. In this way we may study the evolution of the structural properties along other thermodynamic paths, within the disordered phase, besides the one for which only the surfactant concentration is varied at a fixed temperature. The result of the expansion is

$$\begin{aligned} N^{-1}F^{MF} &= N^{-1}F_o^{MF} + \sum_{\mathbf{k}} \Big[\alpha_{\mathbf{k}}\, \eta(-\mathbf{k})\, \eta(\mathbf{k}) + \beta_{\mathbf{k}}\, \rho(-\mathbf{k})\, \rho(\mathbf{k}) \\ &\quad + \gamma_{\mathbf{k}} \Big(\eta(\mathbf{k})\, \rho(-\mathbf{k}) + \eta(-\mathbf{k})\, \rho(\mathbf{k}) \Big) \Big] \ , \end{aligned} \tag{38}$$

with coefficients given by

$$\begin{aligned} \alpha_{\mathbf{k}} &= \frac{T\,\rho_o}{2(\rho_o^2 - \eta_o^2)} - J\,\lambda_1(\mathbf{k}) - (1-\rho_o)\Big[J_1 + 2\,\rho_o\, J_5 \\ &\quad + \rho_o^2\, J_7 + \eta_o^2\, J_8 \Big]\, \lambda_2(\mathbf{k}) - 2\,(1-\rho_o)\,\eta_o^2\, J_8\, \Lambda(\mathbf{k}) \ , \end{aligned} \tag{39}$$

$$\begin{aligned} \beta_{\mathbf{k}} &= \frac{T\,(\rho_o - \eta_o^2)}{2\,(1-\rho_o)\,(\rho_o^2 - \eta_o^2)} - \Big[K - J_2 - 2\,\rho_o\, J_3 - 4\,\rho_o\, J_4 - 2\,\eta_o^2\, J_5 \\ &\quad - 6\rho_o^2 J_6 - 2\rho_o \eta_o^2 J_7 - 2\rho_o^3 J_9 \Big] \lambda_1(\mathbf{k}) - (1-\rho_o)\Big[J_3 + 2\rho_o\, J_6 \\ &\quad + \eta_o^2\, J_7 + \rho_o^2\, J_9 \Big]\, \lambda_2(\mathbf{k}) - 2\,(1-\rho_o)\,\Big[J_4 + 2\,\rho_o\, J_6 + \rho_o^2\, J_9 \Big]\, \Lambda(\mathbf{k}) \ , \end{aligned} \tag{40}$$

$$\begin{aligned} \gamma_{\mathbf{k}} &= -\frac{T\,\eta_o}{2\,(\rho_o^2 - \eta_o^2)} + \eta_o \Big[J_1 + 2\,\rho_o\, J_5 + \rho_o^2\, J_7 + \eta_o^2\, J_8 \Big]\, \lambda_1(\mathbf{k}) \\ &\quad - 2\,(1-\rho_o)\,\eta_o\,[\, J_5 + \rho_o\, J_7 \,]\, \Lambda(\mathbf{k}) \ , \end{aligned} \tag{41}$$

where

$$\lambda_n(\mathbf{k}) = \cos(nk_x) + \cos(nk_y) \;\; ; \Lambda(\mathbf{k}) = 2\cos(k_x)\cos(k_y)\,. \qquad (42)$$

The experimentally important quantities are the water-water, the surfactant-surfactant and the water-surfactant scattering functions, which are respectively defined by

$$S_{WW}(\mathbf{k}) = < \rho^W(-\mathbf{k})\,\rho^W(\mathbf{k}) > \;, \qquad (43)$$

$$S_{SS}(\mathbf{k}) = < \rho^S(-\mathbf{k})\,\rho^S(\mathbf{k}) > \;, \qquad (44)$$

$$S_{WS}(\mathbf{k}) = < \rho^W(-\mathbf{k})\,\rho^S(\mathbf{k}) > \;, \qquad (45)$$

where $\rho^W(\mathbf{k})$ and $\rho^S(\mathbf{k})$ are the $\mathbf{k}^{\text{th}}$ Fourier amplitudes of the fluctuations in the concentrations of water and surfactant around their respective average values. From the definitions $\rho^W(\mathbf{r}) = [\eta(\mathbf{r}) + \rho(\mathbf{r})]/2$ and $\rho^S(\mathbf{r}) = 1 - \rho(\mathbf{r})$, and by means of a standard diagonalization of the bilinear form (38), we obtain

$$S_{WW}(\mathbf{k}) = \frac{1}{4}\left[(1 - A_{\mathbf{k}})\,S^-(\mathbf{k}) + (1 + A_{\mathbf{k}})\,S^+(\mathbf{k})\right] , \qquad (46)$$

$$S_{SS}(\mathbf{k}) = \frac{1}{2}\left[(1 - B_{\mathbf{k}})\,S^-(\mathbf{k}) + (1 + B_{\mathbf{k}})\,S^+(\mathbf{k})\right] , \qquad (47)$$

$$S_{WS}(\mathbf{k}) = -\frac{1}{4}[(1 - A_{\mathbf{k}} - B_{\mathbf{k}})\,S^-(\mathbf{k}) + (1 + A_{\mathbf{k}} + B_{\mathbf{k}})\,S^+(\mathbf{k})], \qquad (48)$$

where

$$A_{\mathbf{k}} = 2\gamma_{\mathbf{k}}/R_{\mathbf{k}} \quad ; \quad B_{\mathbf{k}} = (\beta_{\mathbf{k}} - \alpha_{\mathbf{k}})/R_{\mathbf{k}}$$

$$S^{\pm}(\mathbf{k}) = T\,(\alpha_{\mathbf{k}} + \beta_{\mathbf{k}} \pm R_{\mathbf{k}})^{-1} \quad ; \quad R_{\mathbf{k}} = [(\alpha_{\mathbf{k}} - \beta_{\mathbf{k}})^2 + 4\gamma_{\mathbf{k}}^2]^{1/2}. \qquad (49)$$

The quantities $S^{\pm}(\mathbf{k})$ come from the fact that once the bilinear form is diagonalized, the ensemble distribution is just a simple multivariate Gaussian.

Let us turn our attention to the behavior of the scattering functions along two different thermodynamic paths. First let us consider the case where the mixture is perfectly balanced, that is when $\eta_o = 0$. In this case we have

$$S_{WW} = \frac{1}{4}[S^{-}(\mathbf{k}) + S^{+}(\mathbf{k})] = \frac{T}{8}(\alpha_{\mathbf{k}}^{-1} + \beta_{\mathbf{k}}^{-1}) , \tag{50}$$

$$S_{SS} = S^{+}(\mathbf{k}) = \frac{T}{2}\beta_{\mathbf{k}}^{-1} \quad \text{and} \quad S_{WS} = -\frac{1}{2}S_{SS} . \tag{51}$$

Although the function S_{WW} is a linear combination of $S^{-}(\mathbf{k})$ and $S^{+}(\mathbf{k})$ it is not difficult to see that the contributions from $S^{+}(\mathbf{k})$ to the water-water scattering intensities are much smaller than those from $S^{-}(\mathbf{k})$ in the low surfactant concentration regime, which is the regime of interest. This stems from the factor $\rho^S = 1 - \rho_o$ in the denominator of the first term in the expression for $\beta_{\mathbf{k}}$ (equation 40). Because of the temperature dependence of the couplings J_i it is not simple to extract much information on the behavior of S^{+} and S^{-} as functions of T and ρ^S in an analytical way. However, a straightforward numerical procedure shows that S^{+} is a monotonically decreasing function of $\mathbf{k}$ (inside the Brilloin zone) for almost the entire portion of the phase diagram where the system is disordered. (For high surfactant concentrations S^{+} may increase with k.) This implies that the surfactant-surfactant scattering function has a maximum at zero wavevector and decreases monotonically with $\mathbf{k}$ in that phase. Similar procedure for the function S^{-} shows that it may or may not decrease monotonically with its argument. Therefore, depending on

the values of T and ρ^S, the water-water function can either have a maximum at $\mathbf{k} = 0$ or at some other non-zero value of $\mathbf{k}$. The location of its maximum is given by the equation

$$\left[J + 4\,\rho^S \left(J_1 + 2\,(1-\rho^S)\,J_5 + (1-\rho^S)^2\,J_7 \right) \cos(k) \right] \sin(k) \;=\; 0 \;. \qquad (52)$$

Here $\mathbf{k}$ has been taken along direction $(1,1)$. At a fixed temperature the maximum is located at $k_m = 0$ provided the surfactant concentration is smaller than ρ_S^* given by the solution of

$$J_7\,\rho_S^*\,(1-\rho_S^*)^2 + 2\,J_5\,\rho_S^*\,(1-\rho_S^*) + J_1\,\rho_S^* + J/4 \;=\; 0 \qquad (53)$$

When $\rho^S > \rho_S^*$ the maximum appears at $k_m \neq 0$. As we increase ρ^S the position k_m of the maximum moves towards larger values of k according to

$$k_m \;=\; \arccos\left\{ -J \left[4\rho^S \left(J_1 + 2\,(1-\rho^S)\,J_5 + (1-\rho^S)^2\,J_7 \right) \right]^{-1} \right\} \;. \qquad (54)$$

Equation (53) defines then a line in the disordered phase across which S_{WW} change its behavior with respect to the wavevector. This line is denoted Lifshitz line [1]. In the phase diagram we have shown in Figure 3 the Lifshitz line is the dotted one. To the left of it the fluid is ordinarily disordered with monotonically decreasing scattering functions. To the right of the Lifshitz line the fluid is still disordered, but not *structureless*. The water-water scattering function indicates the presence of structure at a length scale of the order of k_m^{-1}. It is this fluid that many authors have recently identified with the microemulsion. There is no thermodynamic phase transition across this line; the free energy and the scattering functions are all smooth across it.

In Figures 4 and 5 we show the scattering functions S_{WW} and S_{SS}, in arbitrary units, for the same balanced system of Figure 3 at a temperature $T/J = 2.8$. The curves are labeled by their surfactant concentration ρ^S, which are all located to the right of the Lifshitz line. The wavevector k, in units of inverse lattice spacing, is along the direction $(1,1)$. Each function S_{WW} shown in Figure 4 exhibits a peak at non-zero values of wavevector. Its position moves away from zero and its intensity decreases as the surfactant concentration increases along the isotherm $T/J = 2.8$. The intensity of the peak, however, may increase as we get closer to the transition to the lamellar phase, where it actually diverges. The surfactant-surfactant scattering functions S_{SS} are all monotonically decreasing functions with maximum at $k_m = 0$. Their amplitudes are about one order of magnitude smaller than those of S_{WW}. These results are in qualitative agreement with well-known experimental data [32,35]. Figures 4 and 5 are to be qualitative compared with results from references such as [32,35]. Notice, however, that we have to use somewhat larger values of ρ^S in order to be on the right of the Lifshitz line, and hence, to reproduce the desired features. This is consequence of the fact that our calculations were done for a two dimensional system. The values of the peak position k_m can be estimated using the length of the surfactant molecule (typically of the order of $25\mathring{A}$) as the unit of our lattice spacing, which is, of course, a molecular length for the model. The peaks are located around the value $k_m \approx 1.0$, which gives a very reasonable physical value of $4.0 \times 10^{-2}\mathring{A}^{-1}$. This corresponds to domains of water (and oil) of the order of $150\mathring{A}$.

Next we consider the same system, but we take the microemulsion phase

out of balance by allowing for values of η_o different from zero. The thermodynamic path taken is the one for which the temperature is fixed at $T/J = 2.8$, the surfactant concentration is held constant at $\rho^S = 0.2$, and the only parameter allowed to change is the oil fraction ϕ, defined as the ratio of oil to oil plus water. Now, because of the contributions of both S^- and S^+, all scattering functions, including S_{SS}, may present a peak at $\mathbf{k} \neq 0$. The most interesting behavior, however, is exhibited by the water-surfactant scattering function S_{WS}, which is shown in Figure 6. The curves are now labeled by the oil fraction ϕ. One observes that S_{WS} is positive when there is an excess of oil in the system and it is negative when water is in excess. Following ideas first set forth by Widom [36], it is argued in Ref. [32] that $S_{WS}(0)$ is proportional to the average mean curvature of the microemulsion interfacial surfactant film. The argument, which we shall repeat here, is based on the fact that the surfactant tends to be located at the water-oil internal interfaces, such that in a first approximation, a surfactant concentration fluctuation is proportional to an area fluctuation of the interfacial film. As a water concentration variation is introduced in a volume V the surfactant film must move in order to accommodate such a concentration variation. The resulting area variation in V depends on the film mean curvature. For water-in-oil microemulsion, a water excess means a droplet excess, hence a surfactant excess, therefore $S_{WS}(0)$ (which measures cross correlations between water and surfactant) must be positive. Similarly, for oil-in-water microemulsions $S_{WS}(0)$ must be negative. For bicontinuous microemulsions, which have an average mean curvature equal zero, $S_{WS}(0)$ must be very small. This is expected to occur at an oil fraction

$\phi = 0.5$, i.e. at equal water and oil concentrations. (It follows from the relation $S_{WS} = -0.5 S_{SS}$ at $\phi = 0.5$ that $S_{WS}(0)$ is actually negative for balanced microemulsions, but nevertheless, close to zero due to the small amplitudes of S_{SS}. In Ref. [1] it is suggested that a better indicator of the average mean curvature would be$S_{WS} - S_{OS}$ which is identically zero when the system is balanced.)

¿From the results presented in this section it seems that the CHS model, like Schick's model, is able to explain, inter alia, the experimentally observed structural evolution of the microemulsion phase as the ratio of water to oil is driven away from unity in both directions. Finally, the scaled quantity $k^4 S_{WS}$ is plotted against k^2 in Figure 7, where the curves are labeled according to their oil fractions ϕ. This figure shows once again a reassuring resemblance with the experimental data presented in Ref. [32].

7 Site-Correlated Percolation in Ternary Mixtures

In this section we focus on the study of some percolation phenomena in lattice models for microemulsions. In particular, we are interested in the clustering properties of the disordered phase, of which the microemulsion phase is a part. In the last section we saw that, like in Schick's model, the disordered phase of our model is divided by the Lifshitz line into two regions according to the behavior of the water-water scattering function. Both regions, of course, present no long-range order in the thermodynamic sense. Their structures, however, are distinct from each other. In the higher surfactant concentration

side of the Lifshitz line the oscillatory, non-uniform component of the correlation functions dominate the structure factors (the scattering functions have maxima at non-zero wavevector). At surfactant concentrations lower than the ones defining the Lifshitz line, the non-oscillatory, uniform components come to dominate the structure functions. Furthermore, the calculated water-surfactant structure functions, whose values at zero wavevector are associated with the surfactant film expected mean curvature, indicates a structural inversion from water-in-oil to oil-in-water microemulsions as the relative amount of oil to water is varied in the system. A microemulsion with a bicontinuous structure (zero average mean curvature) is then predicted for equal concentrations of water and oil. Here we would like to investigate clustering of particles in the symmetric ($\rho^W = \rho^O$) subspace of the disordered phase of our effective Hamiltonian as well as of Schick's Hamiltonian and learn about percolative properties of the disordered phases of these models.

Percolation is a critical phenomenum characterized by the onset of formation of macroscopic (infinite) clusters of particles in a many-body system. A cluster is defined as a maximal set of particles connected to each other according to a prescribed definition of connectivity between pairs of particles. A single particle is a cluster of size one by definition. The notion of connectivity is a crucial ingredient in the description of the percolative process one wants to study. It defines how the clusters are formed by specifying when a particle belongs to a given cluster or not. It is convenient to classify connectivity that one defines in a model as being of two types [37]. *Connectivity with certainty*: two particles are automatically connected if they lie within a certain

distance apart (this distance can be, for instance, the lattice spacing). *Connectivity in probability*: two particles, a certain distance apart, are connected with probability p. The notion of connectivity leads naturally to the concept of an "active bond" between two particles. If they are connected we say there is an active bond between them and vice-versa. Furthermore, one can classify percolation as *random* or *correlated* depending whether the particles, or bonds, are randomly distributed over the space or are correlated with each other via some interparticle interaction. In what follows we present briefly a mean-field like approximation to determine density thresholds for each of the species in a ternary mixture of particles. Details of the derivation will be published elsewhere [22].

7.1 Equations for the Percolation Thresholds

In order to find the density threshold for a given molecular species l ($l = W, O, S$) we notice that the particles are distributed over the lattice according to a given microemulsion Hamiltonian, from which the thermodynamics and the correlations between particles are assumed to be known. In particular, in the disordered phase of our model the three species of particles are mixed in a homogeneous, isotropic state whose structure functions are known in the mean-field approximation. Connectivity for each molecular species will be defined in a geometrical way, i.e., two particles of the same species are connected if they occupy nearest-neighbor sites on the lattice. There will be many clusters of a given species l. To each of these clusters we randomly associate a $+$ or a $-$ tag.

From our definition of connectivity, it follows that clusters with different tags are not in contact with each other, otherwise both would be forming a single, larger cluster, having a single tag. (This implies that configurations of nearest-neighbor pairs $l^+ - l^-$ are not allowed.) Kikuchi's original approach [38] for the lattice-gas can be easily extended to multicomponent mixtures[22,39] and it is based on the following two theorems[38]: i) *Uniqueness* of the infinite cluster, which says that in a homogeneous, isotropic mixture of particles for which connectivity of a given molecular species is defined, there cannot exits more than one infinite cluster of that particular species; and ii) *Symmetry of Tags*, which says that in the most probable distribution of clusters of a given species the number of + and - clusters of any given finite size are equal to each other. In view of these two theorems, it is clear how to define a percolation order parameter. We divide the particles of species l into three categories. Those belonging to finite + clusters, those belonging to finite − clusters, and those belonging to an infinite, + cluster, with fractions ρ_f^+ , ρ_f^- and ρ_∞^+, respectively. The total number densities of $\pm$-tagged l particles are

$$\begin{aligned} \rho^+ &= \rho_f^+ + \rho_\infty^+ \\ \rho^- &= \rho_f^- . \end{aligned} \tag{55}$$

By the symmetry theorem $\rho_f^+ = \rho_f^-$, therefore

$$\xi \equiv \rho^+ - \rho^- = \rho_\infty^+ \tag{56}$$

is the concentration of particles l belonging to an infinitely extending (isotropic) cluster. That is, ξ is the percolation order parameter for species l, it is non-zero when the species l percolates and zero otherwise.

The thermal distribution of the three species of (untagged) particles is assumed to be known according to the Hamiltonian of the mixture. The most probable distribution of + and − tags among a certain species l is found by maximizing the entropy of the tagged system since neighboring l-particles are connected with probability one. Furthermore, configurations of nearest-neighbor pairs $l^+ - l^-$ are not allowed since all l's in a cluster have the same tag. Percolation occurs when the concentrations of l^+ and l^- are not equal. The entropy of the system, with the l species tagged, is approximated in the pair approximation of the Kikuchi's Cluster Variational Method [40], which is given by

$$\mathcal{S} = (2d-1)\sum_i \mathcal{L}(\rho^i) - d\sum_i \omega_i \mathcal{L}(Y_i) \ , \tag{57}$$

where $\mathcal{L}(x) \equiv x \ln x$. The quantities Y_{ab} are the fractions of nearest-neighbor pairs of particles a and b; ω_i denotes the multiplicity of a given configuration i. Let us investigate clustering of the surfactant species, so that the S-molecules are tagged with either a + or a − tag. Single site and pair configurations are summarized in Table 1. The concentrations are denoted ρ, with $\rho^S = \rho^+ + \rho^-$, and are subject to the constraint $\rho^W + \rho^O + \rho^S = 1$. From Table 1, we obtain

$$\begin{aligned}
\mathcal{S} \ = \ & (2d-1)\left[\rho^W \ln \rho^W + \rho^O \ln \rho^O + \rho^+ \ln \rho^+ + \rho^- \ln \rho^-\right] \\
& -d\Big[Y_{WW} \ln Y_{WW} + Y_{OO} \ln Y_{OO} + 2Y_{WO} \ln Y_{WO} \\
& +2Y^+_{WS} \ln Y^+_{WS} + 2Y^+_{OS} \ln Y^+_{OS} \\
& +2Y^-_{WS} \ln Y^-_{WS} + 2Y^-_{OS} \ln Y^-_{OS} \\
& +Y^{++} \ln Y^{++} + Y^{--} \ln Y^{--}\Big] \ .
\end{aligned} \tag{58}$$

The fractions ρ and Y are geometrically related to each other. The fractions

of water and oil molecules are respectively given by

$$\begin{aligned} \rho^W &= Y_{WW} + Y_{WO} + Y^+_{WS} + Y^-_{WS} \,, \\ \rho^O &= Y_{OO} + Y_{WO} + Y^+_{OS} + Y^-_{OS} \,. \end{aligned} \tag{59}$$

Similarly, the total fraction of tagged surfactant molecules are

$$\begin{aligned} \rho^+ &= Y^+_{WS} + Y^+_{OS} + Y^{++} \,, \\ \rho^- &= Y^-_{WS} + Y^-_{OS} + Y^{--} \,. \end{aligned} \tag{60}$$

We also have

$$\begin{aligned} Y_{WS} &= Y^+_{WS} + Y^-_{WS} \,, \\ Y_{OS} &= Y^+_{OS} + Y^-_{OS} \,, \end{aligned} \tag{61}$$

where the quantities $Y_{WW}, Y_{OO}, Y_{SS}, Y_{WO}, Y_{WS}$ and Y_{OS} are all obtained from the ensemble distribution dictated by the Hamiltonian model. The percolation order parameter is obtained by subtracting equations (60)

$$\xi \equiv \rho^+ - \rho^- = \xi_W + \xi_O + Y^{++} - Y^{--} \,, \tag{62}$$

where

$$\xi_W \equiv Y^+_{WS} - Y^-_{WS} \;\text{ and }\; \xi_O \equiv Y^+_{OS} - Y^-_{OS} \,. \tag{63}$$

The natural independent variables for the percolation transition are ξ, ξ_W and ξ_O. The entropy of the tagged system is then maximized with respect to these variables. The line of percolation threshold for the surfactant species is then given by the solution of

$$\rho^S = \frac{2d-1}{2d-2}(Y_{WS} + Y_{OS}) \,. \tag{64}$$

Similarly, one obtains the threshold lines for water and oil

$$\begin{aligned} \rho^W &= \frac{2d-1}{2d-2}(Y_{WO}+Y_{WS}) \ , \\ \rho^O &= \frac{2d-1}{2d-2}(Y_{WO}+Y_{OS}) \ . \end{aligned} \tag{65}$$

Now we are left with the evaluation of the thermal distribution of the molecular species over the lattice, i.e. we need to evaluate the quantities Y_{WO}, Y_{WS} and Y_{OS} as functions of temperature and composition in the disordered phase of the microemulsion model. The quantity Y_{ij} is defined as the fraction of nearest-neighbor pairs of molecules i and j. In a lattice of coordination number z, it is given by

$$Y_{ij} = \lim_{N\to\infty} \frac{1}{zN} \sum_{\mathbf{r}} \sum_{\delta}^{z} < \rho^i(\mathbf{r})\, \rho^j(\mathbf{r}+\delta) > , \tag{66}$$

where the sum in δ goes over all nearest neighbors of site $\mathbf{r}$ and $< \cdots >$ means thermodynamic average. Fourier expanding the local densities $\rho^i(\mathbf{r})$ around their respective average values in the disordered phase,

$$\rho^i(\mathbf{r}) = \rho_o^i + \sum_{\mathbf{k}\neq 0} \rho^i(\mathbf{k}) e^{i\mathbf{k}\,\cdot\,\mathbf{r}} \ , \tag{67}$$

and using the relation $\lim_{N\to\infty} \frac{1}{N} \sum_{\mathbf{k}} \cdots = \int_{B.Z} \frac{d^dk}{(2\pi)^d} \cdots$, we obtain

$$Y_{ij} = \rho_o^i\, \rho_o^j + \frac{1}{d} \int_{B.Z} \frac{d^dk}{(2\pi)^d}\, \lambda_1(\mathbf{k})\, S_{ij}(\mathbf{k}) \ . \tag{68}$$

(B.Z stands for Brillouin Zone.) Here, as in section 6, S_{ij} is the structure function given by

$$S_{ij}(\mathbf{k}) = < \rho^i(\mathbf{k})\, \rho^j(-\mathbf{k}) > \ , \tag{69}$$

and $\lambda_n(\mathbf{k}) = \sum_{i=1}^{d} \cos(n\, k_i)$. Using equation (67) and the relations

$$\begin{aligned} S_{WO} + S_{WS} &= -S_{WW} \quad , \\ S_{WO} + S_{OS} &= -S_{OO} \quad , \\ S_{WS} + S_{OS} &= -S_{SS} \end{aligned} \tag{70}$$

in equations (63) and (64), we obtain the following equation for the percolation density threshold of a given species l

$$[\rho^l]^2 - \frac{1}{2d-1}\,\rho^l + G_{ll}(T,\rho^l) \;=\; 0\;, \quad l = W,O,S\,, \tag{71}$$

where

$$G_{ll}(T,\rho^l) \;=\; \frac{1}{d}\int_{-\pi}^{\pi} \frac{d^d k}{(2\pi)^d}\,\lambda_1(\mathbf{k})\,S_{ll}(\mathbf{k}) \;. \tag{72}$$

At finite temperatures, equation (71) must be solved numerically. Furthermore, this equation yields meaningful approximated values for the thresholds for any temperature as long as the system is in a disordered, isotropic thermodynamic state.

7.2 Results for Two Lattice Models of Microemulsion

In this section we present results for the spin-1 effective Hamiltonian formulation of the CHS model on a two dimensional square lattice, and for the Schick model on a cubic lattice. [One must bear in mind that we are concerned here with a mean-field description of percolation in lattice systems. In more rigorous theories [41,42,43] the nature of two dimensional lattices imposes serious restrictions on the clustering properties.] The structure functions

for the effective Hamiltonian were calculated in section 6 within a mean-field approximation. For the Schick model they can be calculated exactly in the same way and can be found in reference [3]. (Our $\mathcal{H}_{\text{eff}}$ reduces to the Schick Hamiltonian if one keeps only the couplings J, K and J_3, setting J_3 equal to a temperature-independent L, and disregarding all the others.)

As one can see from equation (70), water and oil percolate simultaneously when both species have same concentration since ,in this case, $S_{WW}(\mathbf{k}) = S_{OO}(\mathbf{k})$. The results for the 2-d symmetric ($H = 0$) effective Hamiltonian with $c/J = 6.0$and $K/J = 3.0$ are shown in Figure 8, where we have used equation (37) in order to obtain the threshold lines in the (T, Δ)-plane. The line labeled S is the percolation locus for the surfactant species. To the left of this line the surfactant particles do not percolate, to its right there is an infinite, isotropic cluster of neighboring surfactant molecules (i.e. the surfactant species is percolating). The line labeled W/O is the simultaneous percolation locus for water and oil molecules. Infinite, isotropic clusters of water and oil exist only to the left of this line. This suggests that the bicontinuous microemulsion should be identified as the region of the disordered phase bounded by these two lines. In this region the system presents three infinite, isotropic ,intertwined clusters of water, oil and surfactant molecules. As the temperature is lowered the percolating network orders into a lamellar phase. There are evidently many finite size clusters for each molecular species, however, their average size distribution and other properties of interest can not be obtained with the treatment presented here. In Figure 9 we show the results for the symmetric (H=C=0) Schick model with $L/J = -3.5$ and $K/J = 0.5$. Similar features

are observed. In the Schick model its not difficult to obtain the asymptotic behavior for the integral G_{ll} (equation 71) in the limit of high temperatures ($\beta \to 0$). In first order in β we obtain from (70) and (71) the following critical values for the percolation transition temperatures. For the surfactant species we have

$$T^S = K \frac{\rho^S(1-\rho^S)^2}{0.2-\rho^S} \ , \ \rho^S < 0.2 \ ; \ d = 3 \ . \tag{73}$$

For water and oil species we have

$$T^{W/O} = 2J \frac{1-\rho^S}{\rho^S - 0.6} \ , \ \rho^S > 0.6 \ ; \ d = 3 \ . \tag{74}$$

Effects from the amphiphilic coupling L in $T^{W/O}$ are present only when second and higher order terms in β are included in the asymptotic expansion of (71). Therefore, to first order in β in the limit of high temperatures, the density thresholds are the same for the Schick and BEG models.

In the next set of figures we display the behavior of the percolation threshold lines with changes in the amphiphilic strength of the surfactant (c in our model, L in Schick's model) as well as with the parameter K, which measures interactions between surfactant molecules in both models (in our model, however, there are other terms of interaction between surfactant particles as given in Appendix A). For illustrative purposes we also include the Lifshitz line in each figure. Figure 10 shows the percolation and the Lifshitz line for the 2-d effective Hamiltonian on the (T, ρ^S)-plane for $K/J = 3.0$ and two values of c (solid and dashed lines correspond to the values $c/J = 6.0$ and $c/J = 4.0$ respectively). The Lifshitz lines are labeled L, surfactant percolation lines are labeled S and the water and oil simultaneous percolation lines are labeled W/O.

For weaker surfactants (smaller values of c) the Lifshitz line moves towards larger values of the surfactant concentration, indicating that it is necessary to have larger amounts of surfactant to induce the usual peaks in the water-water scattering functions, as discussed in section 6. Unlike the Lifshitz line, both the surfactant and the water/oil percolation lines move towards smaller values of their respective density thresholds as the amphiphilic strength c decreases. At the point $T/J = 3.20$, $\rho^s = 0.566$ for the solid W/O percolation line, and at $T/J = 2.21$, $\rho^S = 0.635$ for the dashed W/O percolation line, one observes an abrupt change in the percolation curves indicating ordering of the percolating, disordered phase into a lamellar phase. Figure 11 shows the same physical quantities calculated for the Schick model in three dimensions with $K/J = 0.5$ and two values of L. Solid and dashed lines correspond to $L/J = -3.5$ and $L/J = -1.0$ respectively. The percolation lines are very close to the values given by equations (72) and (73) for the temperature range shown in this figure. ¿From Figures 10 and 11 one observes that the percolation thresholds for our model are relatively more sensitive to the strength of the interactions between surfactant and ordinary particles than they are for the Schick model. The difference in the results of these two models stems from the multi-particle interactions in $\mathcal{H}_{\text{eff}}$ which are not present in Schick's model. The multi-site interactions between surfactants are mostly repulsive, which in turn, disfavor configurations of neighboring surfactant molecules compared to configurations where the surfactant particles are bounded by water and oil. (It is illustrative to observe the coupling energies of the effective Hamiltonian as functions of temperature, which are given in Figure 14.) Hence, a cluster formed by

connected neighbors of surfactant particles percolates at higher thresholds for larger values of the coupling c. These interactions also imply higher thresholds for water or oil clusters for stronger surfactants. We are not aware of any experimental evidence in this regard and it would be interesting to learn how the experimental thresholds change by varying the surfactant strength in a systematic way. However, applying the same formalism to Schick's model, we show, in a separate work [22], that the water percolation threshold for a water-in-oil microemulsion system, increases as a function of the coupling C of that Hamiltonian [3]. That is, the water percolation threshold increases as the surfactant becomes more lipophilic. This is in qualitative agreement with experimental results [44] on water + AOT + undecane, where such a threshold is found to increase with salinity. Recall that by increasing the value of C one can mimic [3] the addition of salt to a system with an ionic surfactant such as AOT [16].

The behavior of the percolation lines for different values of K is shown in Figure 12 for $\mathcal{H}_{\text{eff}}$ with $c/J = 4.0$. Solid and dashed lines correspond to $K/J = 1.0$ and $K/J = 3.0$ respectively. The curves are labeled as before. The same quantities calculated for the Schick model in three dimensions are shown in Figure 13, where the amphiphilic strength is fixed at $L/J = -3.5$. Solid and dashed lines corresponds to $K/J = 0.5$ and $K/J = 1.5$ respectively. Both models show similar features, with higher density thresholds for smaller values of K, as expected from our discussion above.

We end this section with a few remarks in connection with the fact that our calculations are at a mean-field level and as such, they overlook several

important aspects regarding percolative transitions, specially in systems of low dimensionality. First we would like to emphasize that the percolation lines shown in Figures 8, 10 and 12 (effective Hamiltonian on a square lattice) are to be percieved as an example of the qualitative behavior one expects to find at d=3, since more rigorous analyses show that on a square lattice no more than one species can percolate [45]. In these figures we are mainly interested in showing where these thresholds are located in the phase diagram and how they respond to changes in some of the interaction strengths. Second, we point out that the infinite temperature limit of the thresholds we have calculated are not accurate compared to rigorous results; again because the present treatment is of the mean-field type. The same applies to the calculations performed by Kikuchi and also by Murata [38] for the Ising model.

Acknowledgements

G.S. gratefully acknowledges support by the Division of Chemical Sciences, Office of Basic Energy Sciences, Office of Energy Research, U.S. Department of Energy. M.S. is grateful to the National Science Foundation for financial support.

Appendix A

In this Appendix we write the effective Hamiltonian for a two-dimensional square lattice as a polynomial in four variables. In equation (28) we have

$$\mathcal{H}_{\text{eff}} = -\sum_{\mathbf{r}} [1 - S^2(\mathbf{r})] \ln \sum_{j=1}^{d} 2\cosh\left(\beta c [S(\mathbf{r}+\mathbf{e}_j) - S(\mathbf{r}-\mathbf{e}_j)]\right) \quad , \quad (75)$$

where $S(\mathbf{r})$ assume values $0, \pm 1$. Consider now the function

$$h(\mathrm{x}_1, \mathrm{x}_2; \mathrm{y}_1, \mathrm{y}_2) \equiv \ln\left[2\cosh\,\beta c(\mathrm{x}_1 - \mathrm{x}_2) + 2\cosh\,\beta c(\mathrm{y}_1 - \mathrm{y}_2)\right] \quad , \quad (76)$$

which is to be evaluated only at the points x_j and $y_j = 0, \pm 1$, so that $x_j^3 = x_j$ and $y_j^3 = y_j$. Due to this property h can be written as a polynomial in x_j and y_j, where the highest degree of any of the variables can not be greater than two. In order to find such a polynomial one must consider the symmetry transformations under which h is invariant. These are trivially obtained considering the parity of the function cosh. It is not difficult then to see that the polynomial must be of the form

$$\begin{aligned} P(\mathrm{x}_1, \mathrm{x}_2; \mathrm{y}_1, \mathrm{y}_2) \;=\; & J_o + J_1(\mathrm{x}_1\,\mathrm{x}_2 + \mathrm{y}_1\,\mathrm{y}_2) + \frac{1}{2} J_2(\mathrm{x}_1^2 + \mathrm{x}_2^2 + \mathrm{y}_1^2 + \mathrm{y}_2^2) \\ & + J_3(\mathrm{x}_1^2\,\mathrm{x}_2^2 + \mathrm{y}_1^2\,\mathrm{y}_2^2) + J_4(\mathrm{x}_1^2 + \mathrm{x}_2^2)\,(\mathrm{y}_1^2 + \mathrm{y}_2^2) \\ & + J_5[\mathrm{x}_1\,\mathrm{x}_2(\mathrm{y}_1^2 + \mathrm{y}_2^2) + \mathrm{y}_1\,\mathrm{y}_2(\mathrm{x}_1^2 + \mathrm{x}_2^2)] \\ & + J_6[\mathrm{x}_1^2\,\mathrm{x}_2^2(\mathrm{y}_1^2 + \mathrm{y}_2^2) + \mathrm{y}_1^2\,\mathrm{y}_2^2(\mathrm{x}_1^2 + \mathrm{x}_2^2)] \\ & + J_7(\mathrm{x}_1\,\mathrm{x}_2\,\mathrm{y}_1^2\,\mathrm{y}_2^2 + \mathrm{x}_1^2\,\mathrm{x}_2^2\,\mathrm{y}_1\,\mathrm{y}_2) \\ & + J_8\,\mathrm{x}_1\mathrm{x}_2\,\mathrm{y}_1\mathrm{y}_2 + J_9\,\mathrm{x}_1^2\mathrm{x}_2^2\,\mathrm{y}_1^2\mathrm{y}_2^2 \,. \end{aligned} \quad (77)$$

In order to find the coefficients J_i we must solve a 9×9 linear system of equations which is obtained by equating the values of the polynomial P and

the function h at the points x_i and $y_j = 0, \pm 1$. The solution of such a system gi

$$
\begin{aligned}
J_1 &= -\frac{1}{2} \ln \frac{1}{2}(1 + \cosh 2\beta c) \\
J_2 &= 2 \ln \frac{1}{2}(1 + \cosh \beta c) \\
J_3 &= -J_1 - J_2 \\
J_4 &= J_3 \\
J_5 &= -J_1 + \frac{1}{4} J_2 - \frac{1}{2} \ln \frac{1}{2}(\cosh \beta c + \cosh 2\beta c) \\
J_6 &= -2 J_4 - J_5 \\
J_7 &= -J_1 - 2 J_5 - \frac{1}{4} \ln \cosh 2\beta c \\
J_8 &= J_1 + \frac{1}{4} \ln \cosh 2\beta c \\
J_9 &= -4J_4 - 4J_6 + J_8 \ . \qquad (78)
\end{aligned}
$$

Therefore, the effective Hamiltonian for a square lattice is

$$\mathcal{H}_{\text{eff}} = -\sum_{\mathbf{r}} [1 - S^2(\mathbf{r})] \, P[S(\mathbf{r} + \mathbf{e}_x), S(\mathbf{r} - \mathbf{e}_x); S(\mathbf{r} + \mathbf{e}_y), S(\mathbf{r} - \mathbf{e}_y)] \qquad (79)$$

(In our calculation we have left out the term in J_o, since it merely renormalizes the surfactant chemical potential Δ in the full Hamiltonian.) A similar expression can be obtained also in three dimensions, in this case we have a polynomial with

The couplings J_2, J_5 and J_6 are positive, while all the other are negative. All of them tend to zero in the limit $T/c \to \infty$. In Figure 14 we show the temperature dependence of the coupling energies.

References

[1] G. Gompper and M. Schick, *Phys. Rev. Lett.* **62**, 1647 (1989).

[2] G. Gompper and M. Schick, *Phys. Rev. Lett.* **65**, 1116 (1990).

[3] G. Gompper and M. Schick, *Phys. Rev. B* **41**, 9148 (1990).

[4] K. A. Dawson, M. D. Lipkin and B. Widom, *J. Chem. Phys.* **88**, 5194 (1988).

[5] B. Widom, *J. Chem. Phys.* **90**, 2437 (1989).

[6] G. M. Carneiro and M. Schick, *J. Phys. Chem.* **89**, 4368 (1988).

[7] A. Ciach, J. S. Høye and G. Stell, *J. Phys. A* **21**, L777 (1988); *J. Chem. Phys.* **90**, 1214 (1989); **95**, 5300 (1991).

[8] A. Ciach and J. S. Høye, *J. Chem. Phys.* **90**, 1222 (1989).

[9] A. Ciach, *J. Chem. Phys.* **93**, 5322 (1990) .

[10] A. Ciach, J. Høye and G. Stell,*J. Chem. Phys.***95**, 5300 (1991).

[11] L. Renlie, J. Høye, M. Skaf and G. Stell, *J. Chem. Phys.* **95**, 5305 (1991).

[12] M. W. Matsen and D. E. Sullivan, *Phys. Rev. A* **41**, 2021 (1990).

[13] M. W. Matsen and D. E. Sullivan, *Phys. Rev. A* **44**, 3710 (1991).

[14] M. W. Matsen and D. E. Sullivan, *J. Physique II* **2**, 93 (1992).

[15] M. Laradji, H. Guo, M. Grant and M. Zuckermann, *Phys. Rev. A* **44**, 8184 (1991).

[16] K. Shinoda, B. Lindman, *Langmuir* **3**, 135 (1987).

[17] M. Kahlweit and R. Strey, *Angew. Chem. Int.* (Ed. Engl.) **24**, 654 (1985); see also in *Microemulsion Systems*, edited by H. L. Rosano and M. Clausse (Marcel Dekker, N.Y. 1987).

[18] M. Kahlweit et al., *Langmuir* **1**, 281 (1985).

[19] G. J. Tiddy, *Phys. Rep.* **57**, 1 (1980).

[20] M. Schick and W. H. Shih, *Phys. Rev. Lett.* **59**, 1205 (1987); *Phys. Rev. B* **34**, 1797 (1986).

[21] G. Gompper and M. Schick, in *Modern Ideas and Problems in Amphiphilic Science*, edited by W. M. Gelbart, D. Roux and A. Ben-Shaul (Springer-Verlag, Berlin, in press).

[22] Munir S. Skaf and George Stell, *Phys. Rev. A*, to appear.

[23] M. Blume, V. J. Emery and R. B. Griffiths, *Phys. Rev. A* **4**, 1071 (1971).

[24] J. W. Halley and A. J. Kolan, *J. Chem. Phys.* **88**, 3313 (1988).

[25] G. Gompper and M. Schick, *Chem. Phys. Lett.* **163**, 475 (1989).

[26] J. Alexander, *J. Physique Lett.* **39**, L 1 (1978).

[27] J. C. Wheeler and B. Widom, *J. Am. Chem. Soc.* **90**, 3064 (1968); B. Widom, *J. Phys. Chem.* **88**, 6508 (1984).

[28] D. Mukamel and M. Blume, *Phys. Rev. A* **10**, 610 (1974).

[29] S. A. Brazovskii, *Sov. Phys. JETP* **41**, 85 (1975).

[30] B. Widom, *J. Chem. Phys.* **84**, 6943 (1986).

[31] K. Chen, C. Ebner, C. Jayaprakash and R. Pandit, *J. Phys. C* **20**, L361 (1987); *Phys. Rev. A* **38**, 6240 (1988).

[32] L. Auvray, J. P. Cotton, R. Ober and C. Taupin, *J. Phys.* **45**, 913 (1984); *J. Phys. Chem.* **88**, 4586, (1984); *Physica* **136 B**, 281 (1986).

[33] M. Kotlarchick, S.-H. Chen, J.S. Huang and M. W. Kim, *Phys. Rev. Lett.* **43**, 941 (1984).

[34] C. G. Vonk, J. F. Billman and E. W. Kaler, *J. Chem. Phys.* **88**, 3970 (1988).

[35] M. Teubner and R. Strey, *J. Chem. Phys.* **87**, 3195 (1987).

[36] B. Widom, *J. Chem. Phys.* **81**, 1030 (1984) .

[37] J. Xu and G. Stell, *J. Chem. Phys.* **89**, 1101 (1988).

[38] R. Kikuchi, *J. Chem. Phys.* **53**, 2713 (1970). See also K. Murata, *J. Phys. A***12**, 81 (1979).

[39] Munir S. Skaf, Ph.D. Dissertation, State University of New York at Stony Brook, August 1991.

[40] R. Kikuchi, *Phys. Rev.* **81**, 988 (1951).

[41] M. E. Fisher, *J. Math. Phys.* **2**, 620 (1961).

[42] T. E. Harris, *Proc. Comb. Phil. Soc.* **56**, 13 (1960).

[43] M. Miyamoto,*Comm. Math. Phys.* **44**, 169 (1975).

[44] M. Moha-Ouchane, J. Peyrelasse and C. Boned, *Phys. Rev. A* **35**, 3027 (1987).

[45] J. W. Halley, in *Percolation Structures and Processes* (Annals of the Israel Physical Society, Vol. 5), G. Deutcher, R. Zallen and J. Adler, editors (AIP, New York, 1983).

Table Captions

Table 1. Single site and nearest-neighbor pair configurations with respective fractions and multiplicities. Clustering is sought for the surfactant species. Configurations $S^+ - S^-$ are not allowed.

Figure Captions

Figure 1. Boundary of stability of the disordered phase for a three dimensional cubic lattice using the CHS model with oriented surfactant molecules. To the left of the point $k_c = 0$ the disordered phase undergoes second order transitions into uniform water-rich and oil-rich phases. For higher values of Δ the disordered phase makes transitions into periodically ordered phases. We have used $c/J = 5.5, K/J = 1.0, g = 0$ and $H = 0$.

Figure 2. Critical values of the modulation wavevector as a function of the surfactant concentration along the line shown in Figure 1.

Figure 3. Phase diagram in the (T, Δ)-plane for a two dimensional square lattice using the effective Hamiltonian in its polynomial form with $c/J = 6.0, K/J = 3.0$ and $H = 0$. First order and second order phase transitions are shown by solid and dashed lines respectively. The tricritical point is marked with a full dot. The dotted line indicates the locus of points where the water-water scattering function changes its behavior (Lifshitz line). This is not a line of thermal phase transitions. Coexistence between water/oil-rich and lamellar phases, and between lamellar and 2-d modulated phases are shown schematicaly by solid-dashed lines.

Figure 4. Water-water scattering functions in arbitrary units for the system of Figure 3 held at $T/J = 2.8$ with equal concentrations of water and oil. The curves are labeled by the surfactant concentrations which are all located to the right of the Lifshitz line. The wavevector, in units of inverse lattice spacing, is varied along the direction (1,1).

Figure 5. Surfactant-surfactant scattering functions in arbitrary units along the same thermodynamic path of Figure 4. The curves are labeled by the surfactant concentration. The wavevector, in units of inverse lattice spacing, is varied along the direction (1,1).

Figure 6. Water-surfactant scattering functions for the same system described in Figure 3 held at $T/J = 2.8$ and $\rho^S = 0.2$. The microemulsion is taken out of balance by moving the water to oil concentration ratio away from unity. The curves are labeled by the oil fraction ϕ defined as the oil to oil plus water concentration ratio. The wavevector, in units of inverse lattice spacing, is varied along the direction (1,1).

Figure 7. Scaled water-surfactant scattering functions for the same system as in Figure 6. The curves are again labeled by the oil fraction ϕ.

Figure 8. Location of the percolation threshold lines on the phase diagram for the effective Hamiltonian on a square lattice with $c/J = 6.0$, $K/J = 3.0$ and $H = 0$. The lines labeled S and W/O refer to surfactant and to water and oil thresholds respectively.

Figure 9. Location of the percolation thresholds on the phase diagram for the Schick model in three dimensions with $L/J = -3.5$, $K/J = 0.5$ and $H = C = 0$. The surfactant percolation line is labeled S and the simultaneous water and oil percolation line is labeled W/O. The solid-dashed line is the Lifshitz line. First order phase transitions are shown by solid lines.

Figure 10. Lifshitz lines and percolation thresholds for the symmetric ($H = 0$) effective Hamiltonian with $K/J = 3.0$, $c/J = 6.0$ (solid lines) and $c/J = 4.0$ (dashed lines).

Figure 11. Lifshitz lines and percolation thresholds for the symmetric ($H = C = 0$) 3-d Schick model with $K/J = 0.5$, $L/J = -3.5$ (solid lines) and $L/J = -1.0$ (dashed lines).

Figure 12. Lifshitz and percolation lines for the 2-d effective Hamiltonian with $c/J = 4.0$ and $K/J = 1.0$ for solid lines, and $K/J = 3.0$ for dashed lines. Notice that the Lifshitz lines correponding to $K/J = 1.0$ and $K/J = 3.0$ coincide since the Lifshitz line is independent of K in this approximation.

Figure 13. Lifshitz and percolation lines for the Schick model with $L/J = -3.5$ and $K/J = 0.5$ for solid lines, and $K/J = 1.5$ for dashed lines. Notice that the Lifshitz lines correponding to $K/J = 1.0$ and $K/J = 3.0$ coincide since the Lifshitz line is independent of K in this approximation.

Figure 14. Temperature dependence of the 2-d effective Hamiltonian energy couplings.

Table 1

Configurations	Fractions	Multiplicities ω_i
W	ρ^W	1
O	ρ^O	1
S^+	ρ^+	1
S^-	ρ^-	1
$W-W$	Y_{WW}	1
$W-O$	Y_{WO}	2
$O-O$	Y_{OO}	1
$W-S^+$; $W-S^-$	Y^+_{WS} ; Y^-_{WS}	2 ; 2
$O-S^+$; $O-S^-$	Y^+_{OS} ; Y^-_{OS}	2 ; 2
S^+-S^+	Y^{++}	1
S^--S^-	Y^{--}	1

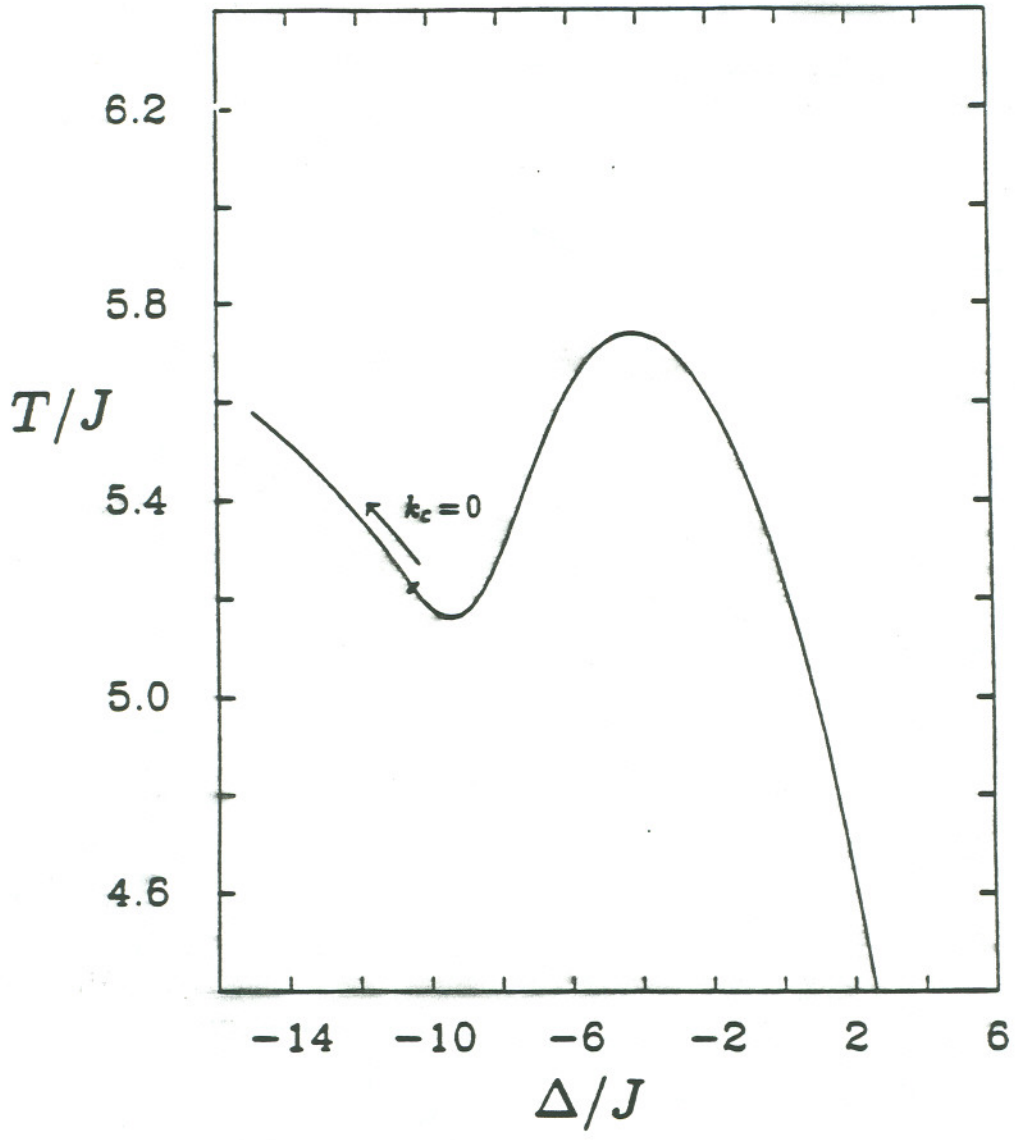

SKAT + STELL Fig. 1

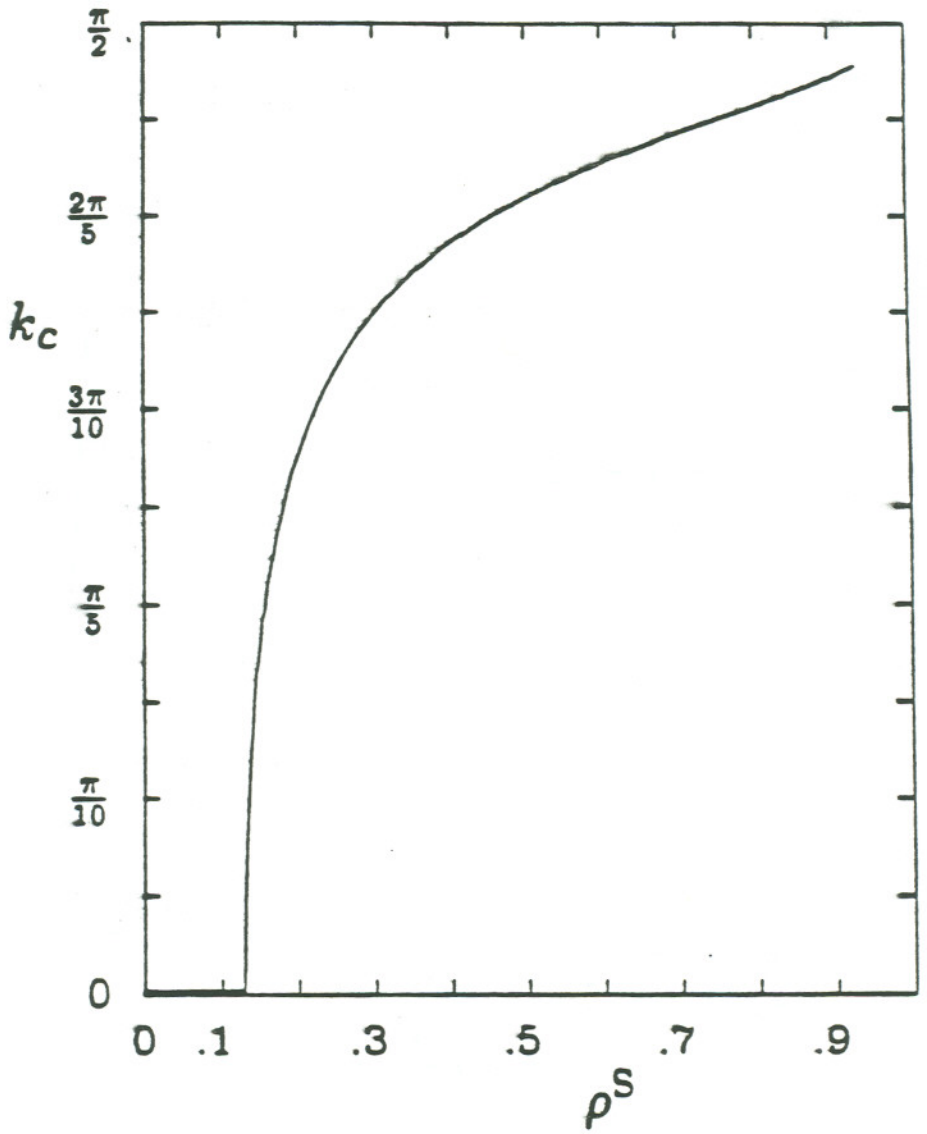
$\frac{\pi}{2}$
$\frac{2\pi}{5}$
k_c
$\frac{3\pi}{10}$
$\frac{\pi}{5}$
$\frac{\pi}{10}$
0
0
.1
.3
.5
.7
.9
ρ^s

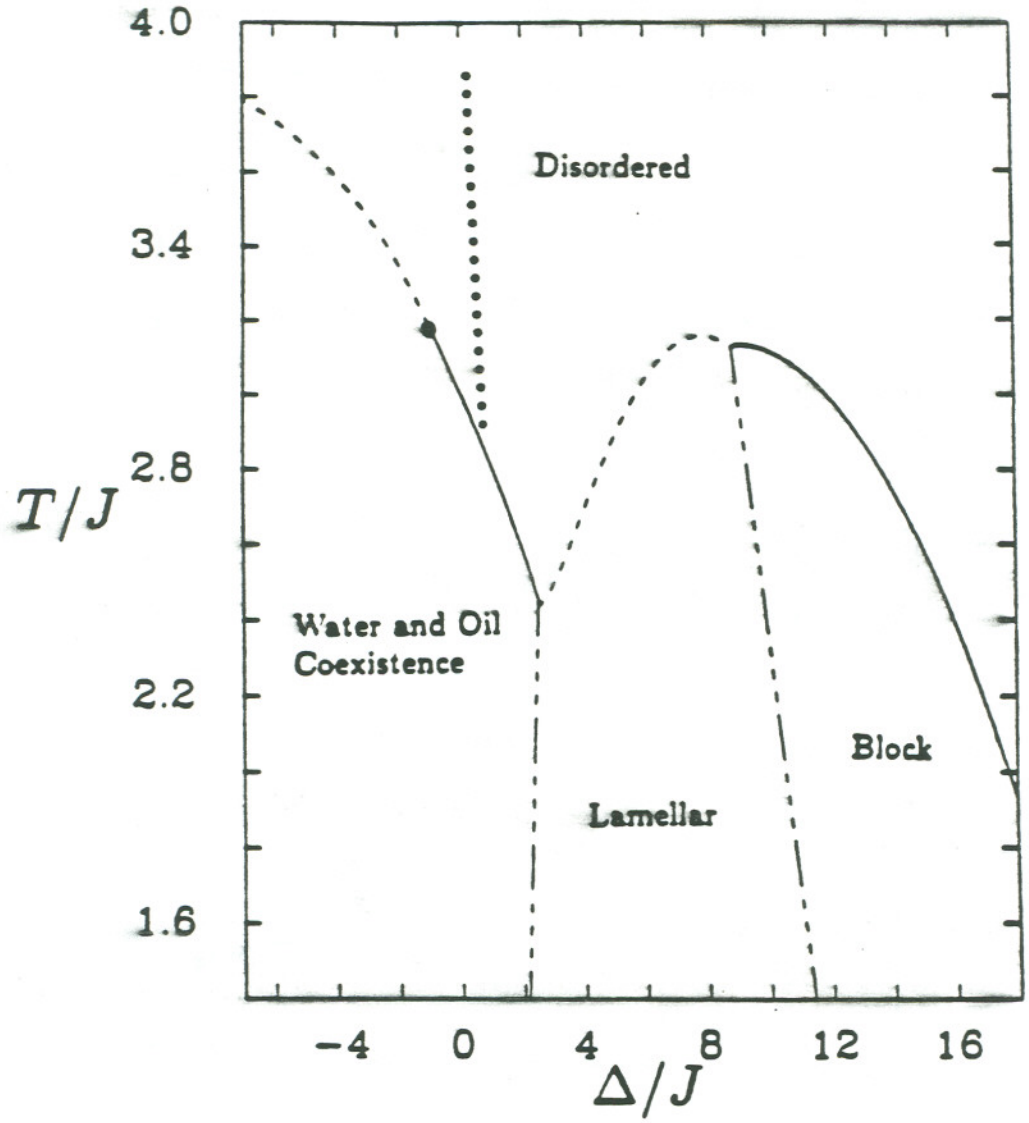
4.0
3.4
2.8
2.2
1.6
T/J
Disordered
Water and Oil
Coexistence
Lamellar
Block
−4
0
4
8
12
16
Δ/J

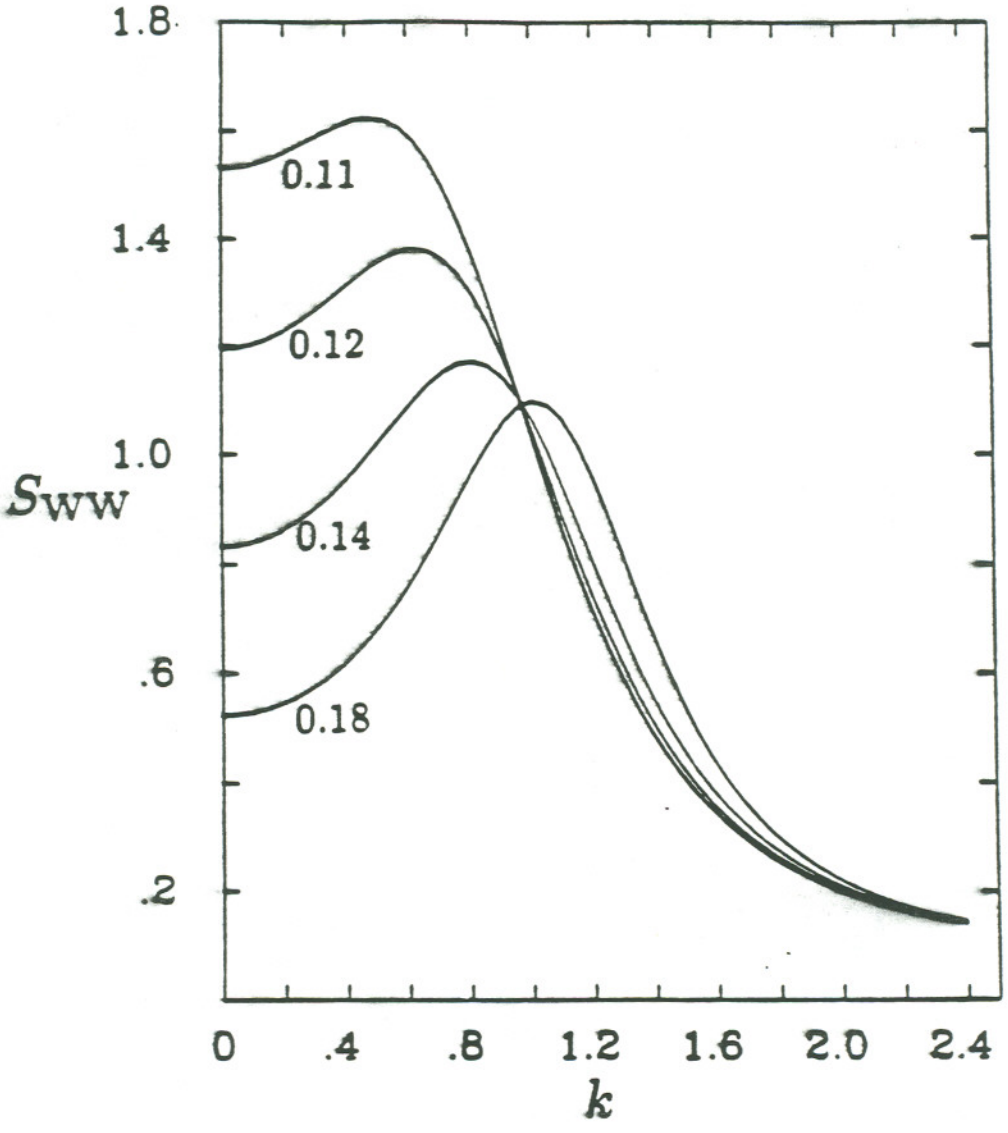

SKAF + STELL Fig. 4

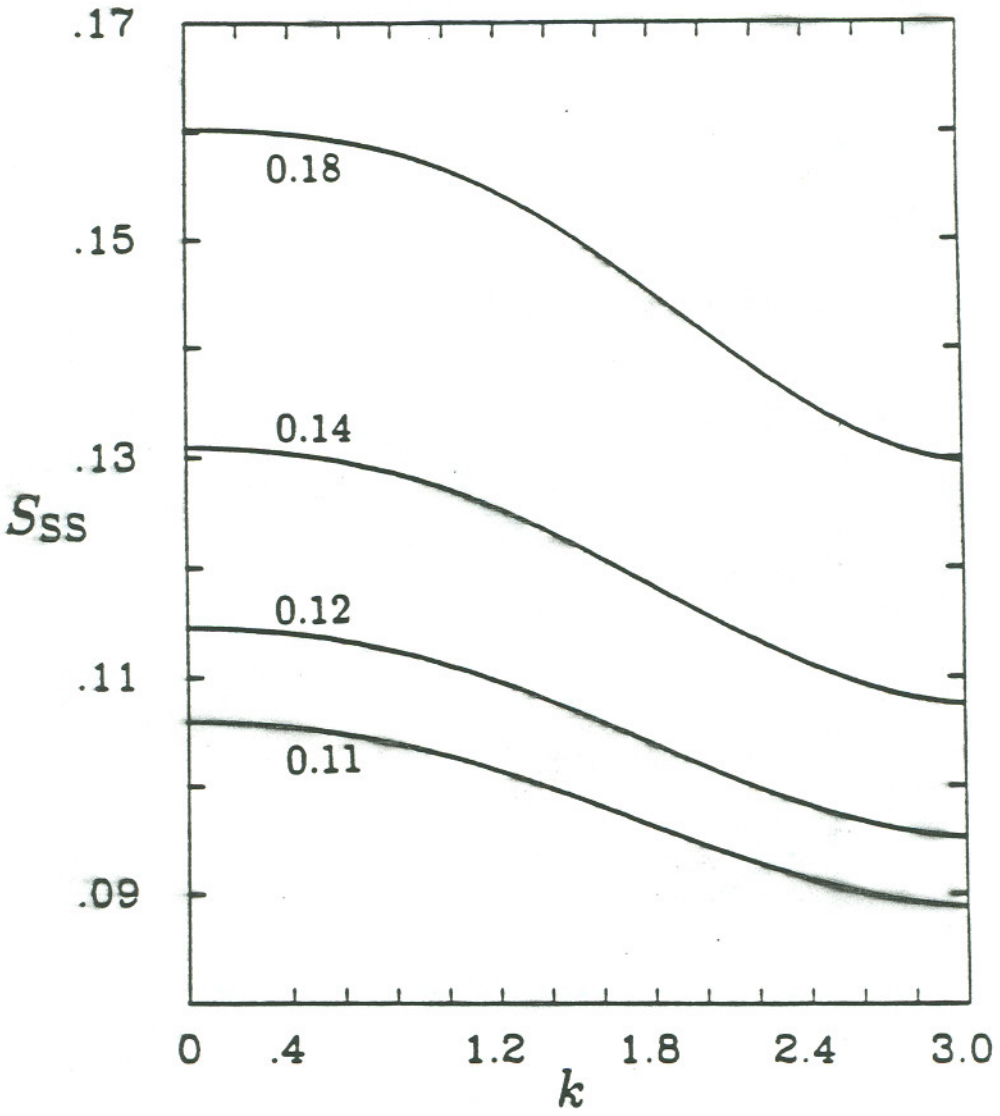

SHAFT STEEL Fig 5

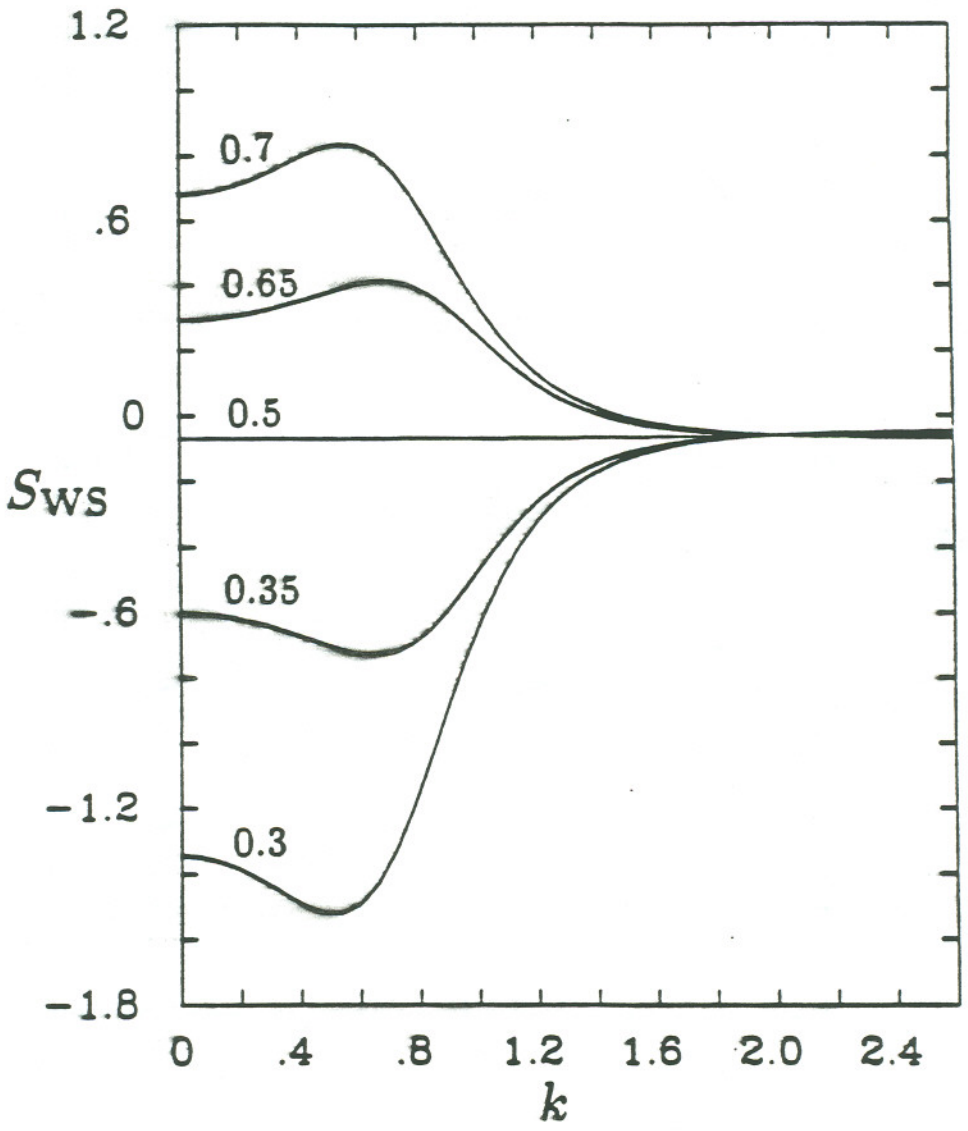

SKAF + STELL Fig. 6

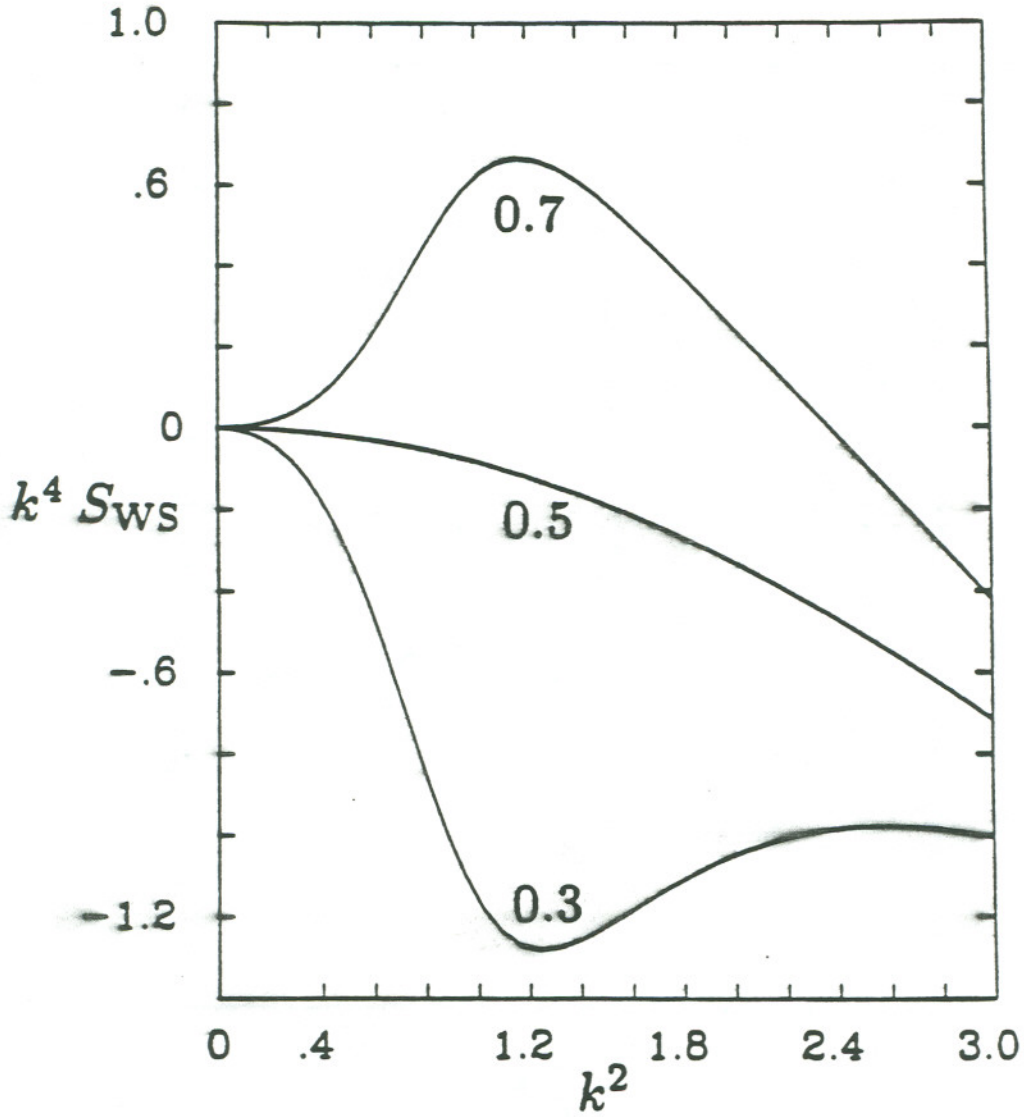
1.0
.6
0
−.6
−1.2
$k^4 S_{WS}$
0.7
0.5
0.3
0
.4
1.2
1.8
2.4
3.0
k^2

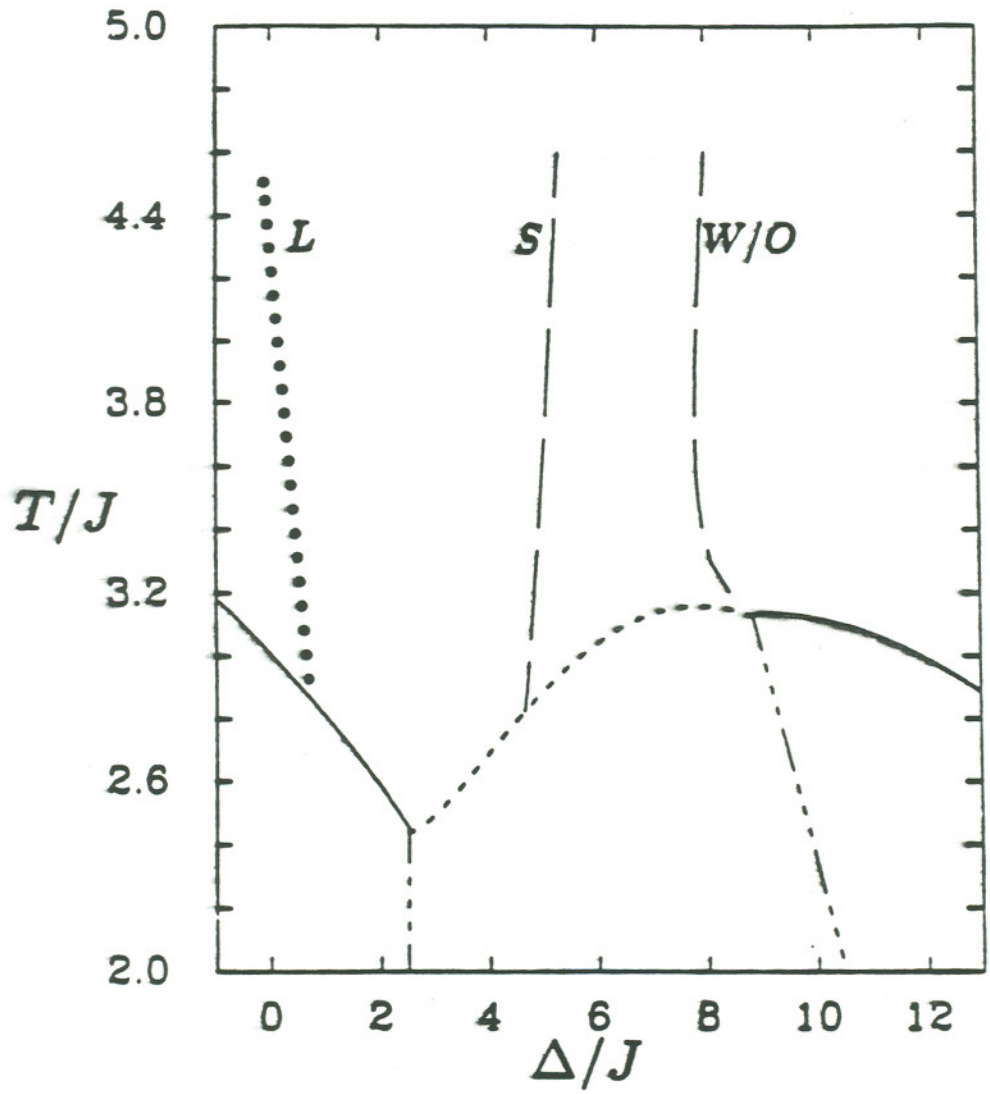

Fig. 8

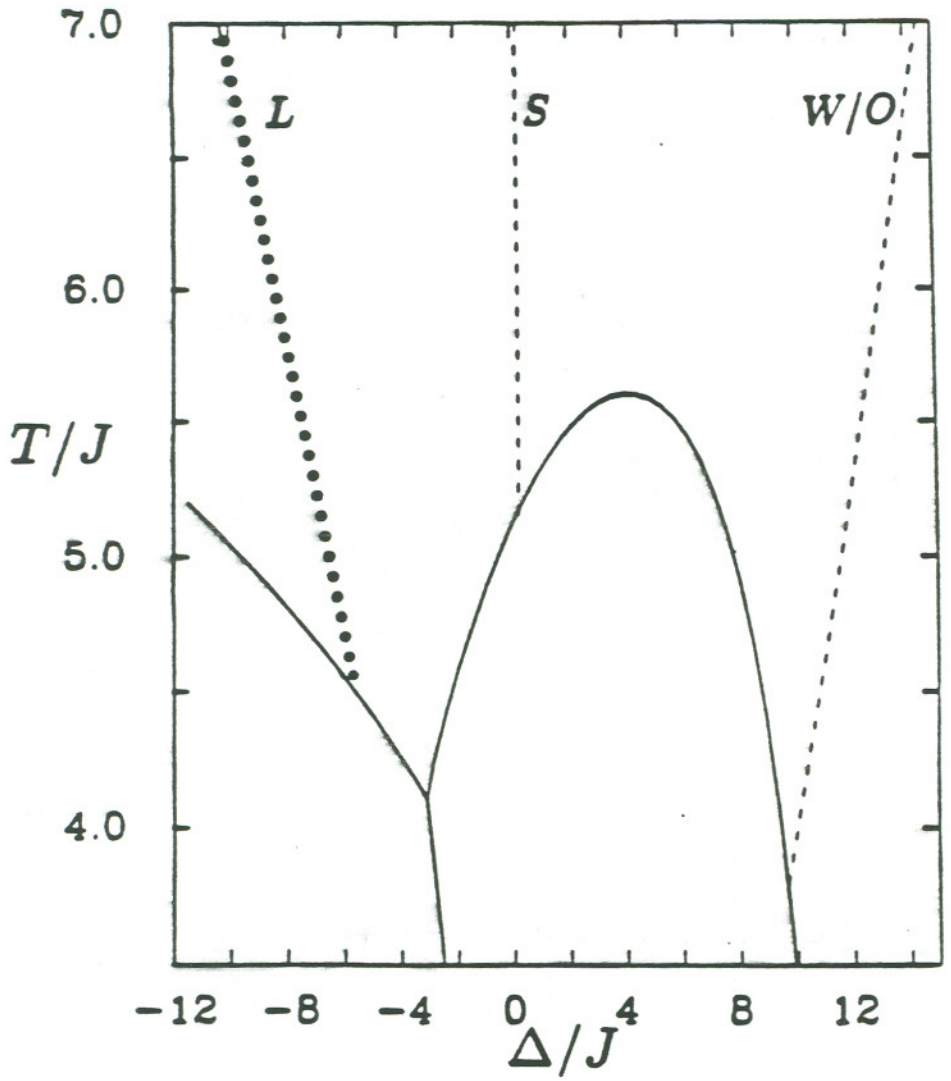

Fig. 9

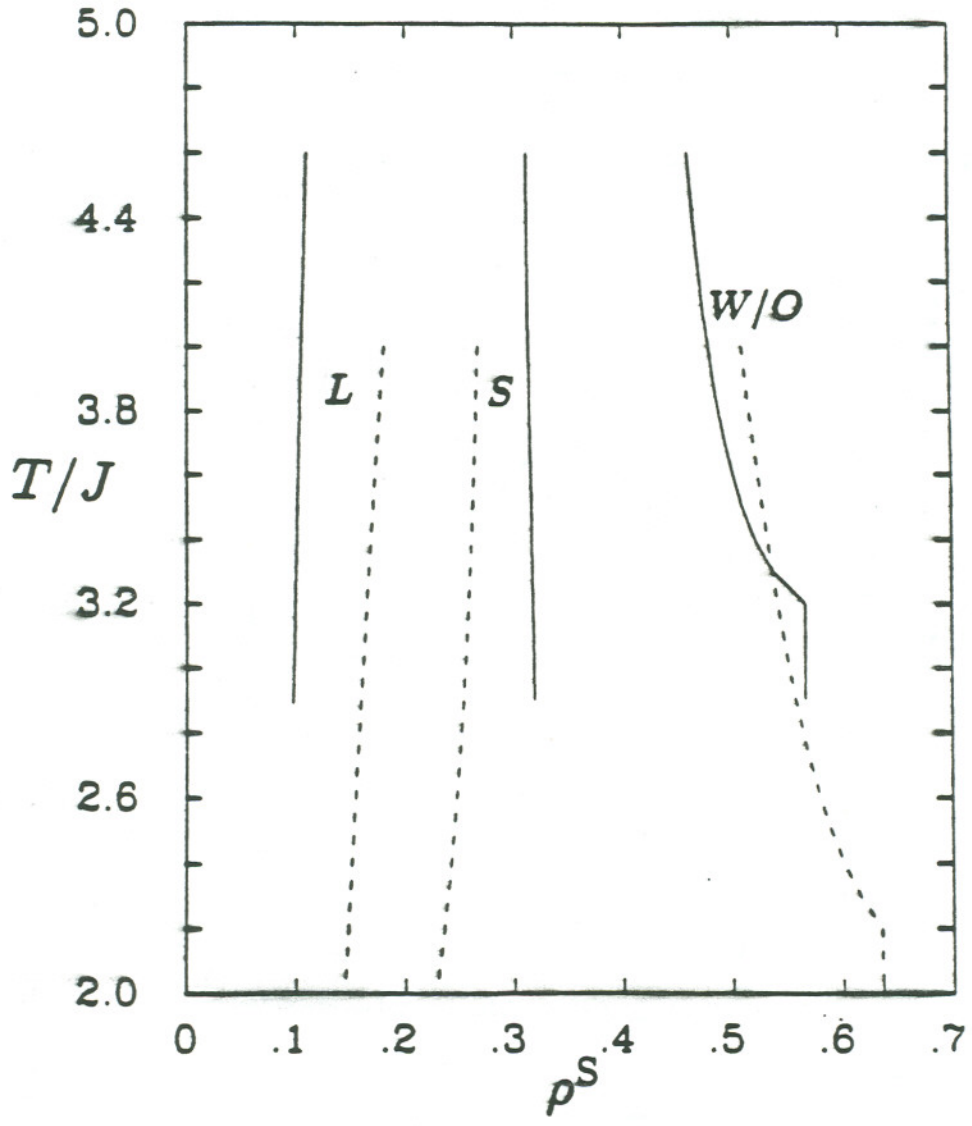

Fig 10

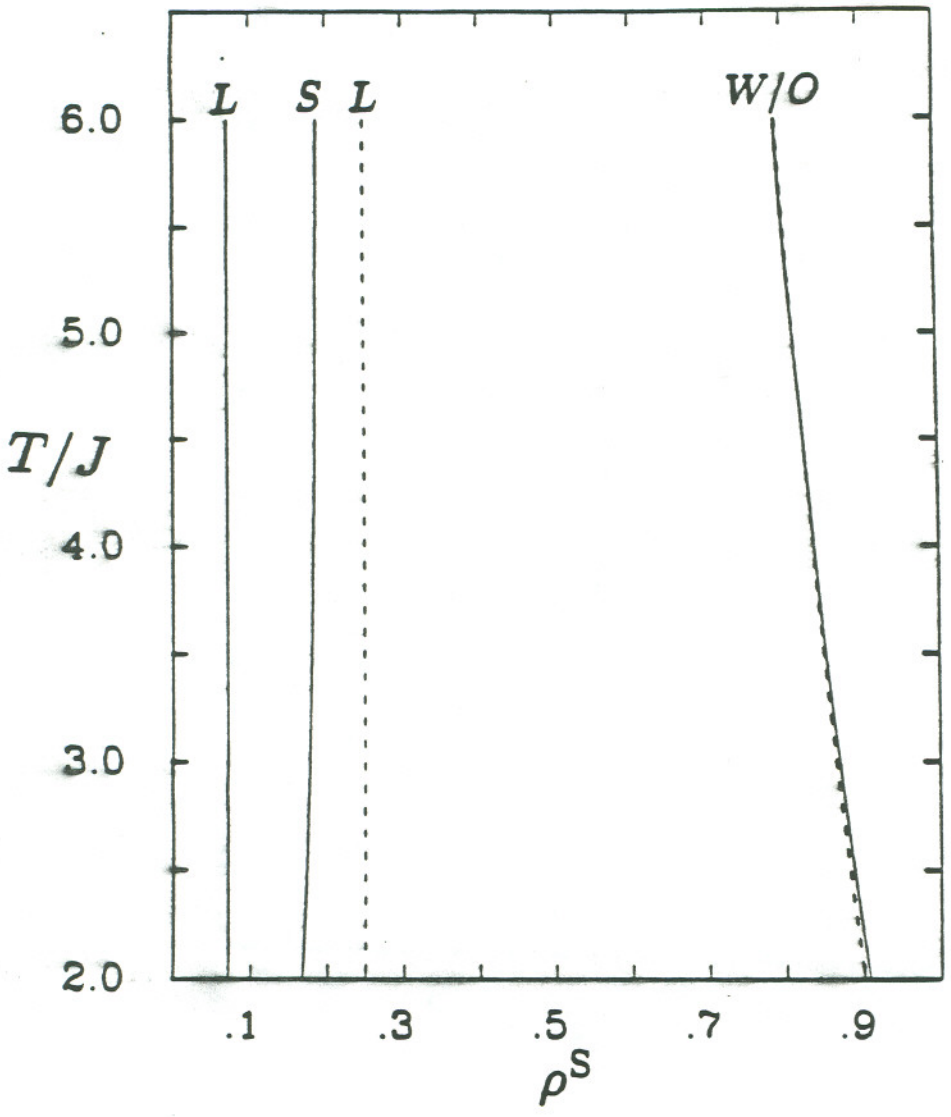

Fig 11

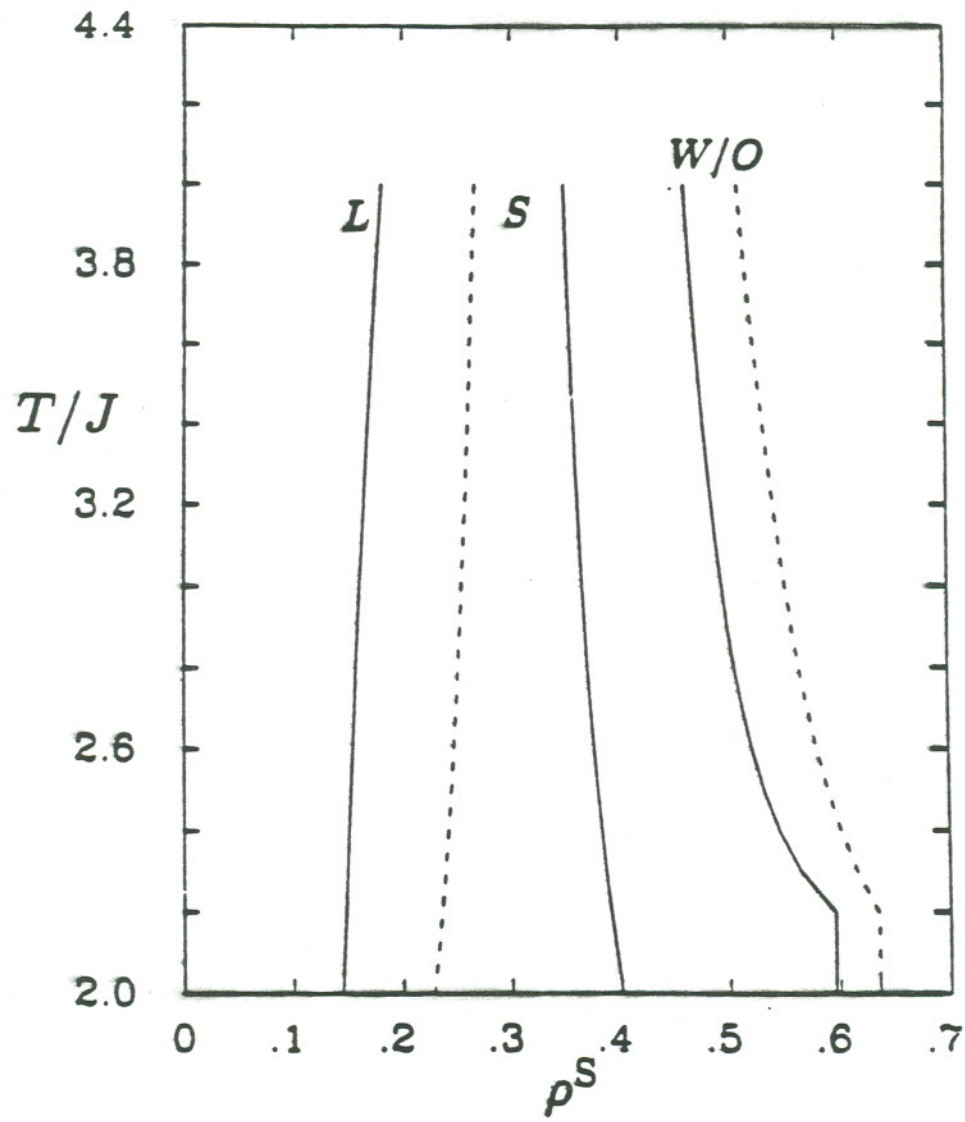

SKAF + STELL Fig. 12

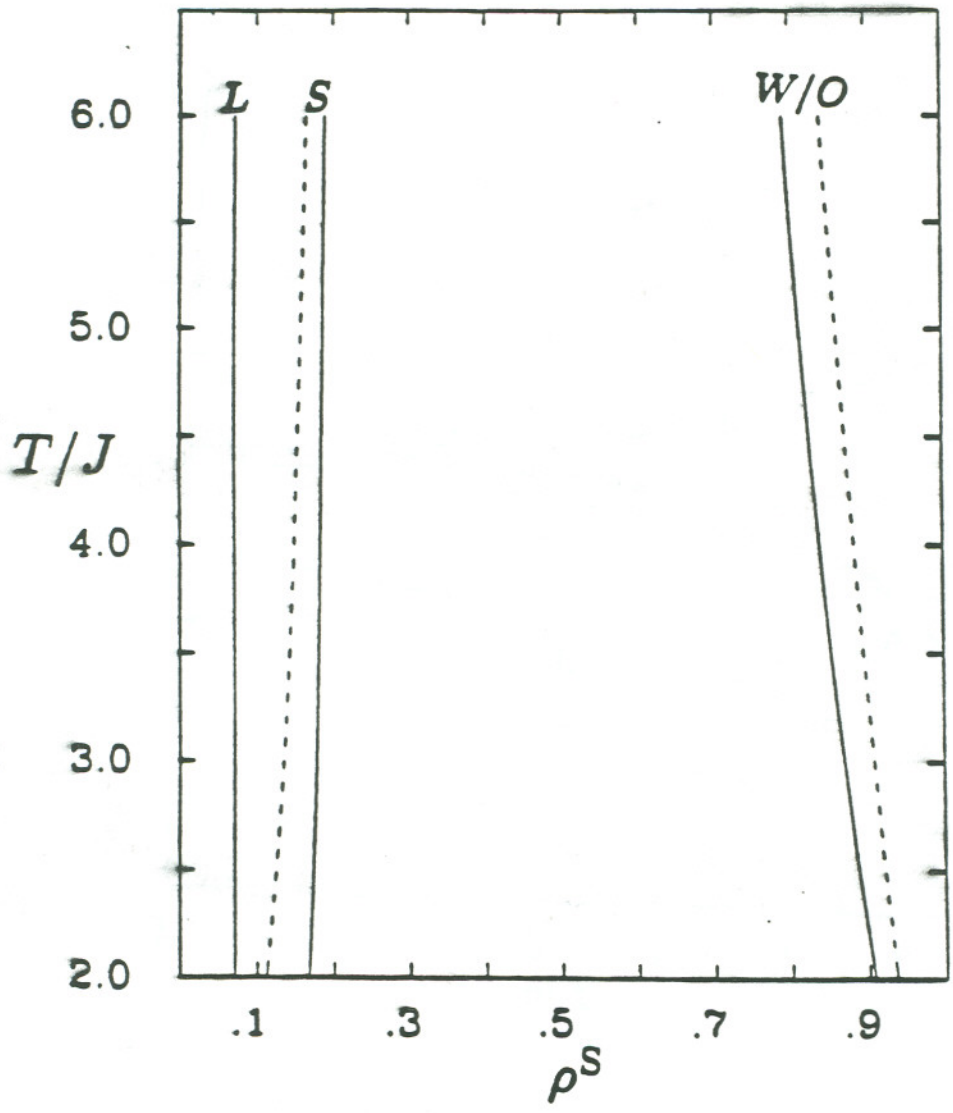
L
S
W/O
6.0
5.0
4.0
3.0
2.0
T/J
.1
.3
.5
.7
.9
ρS

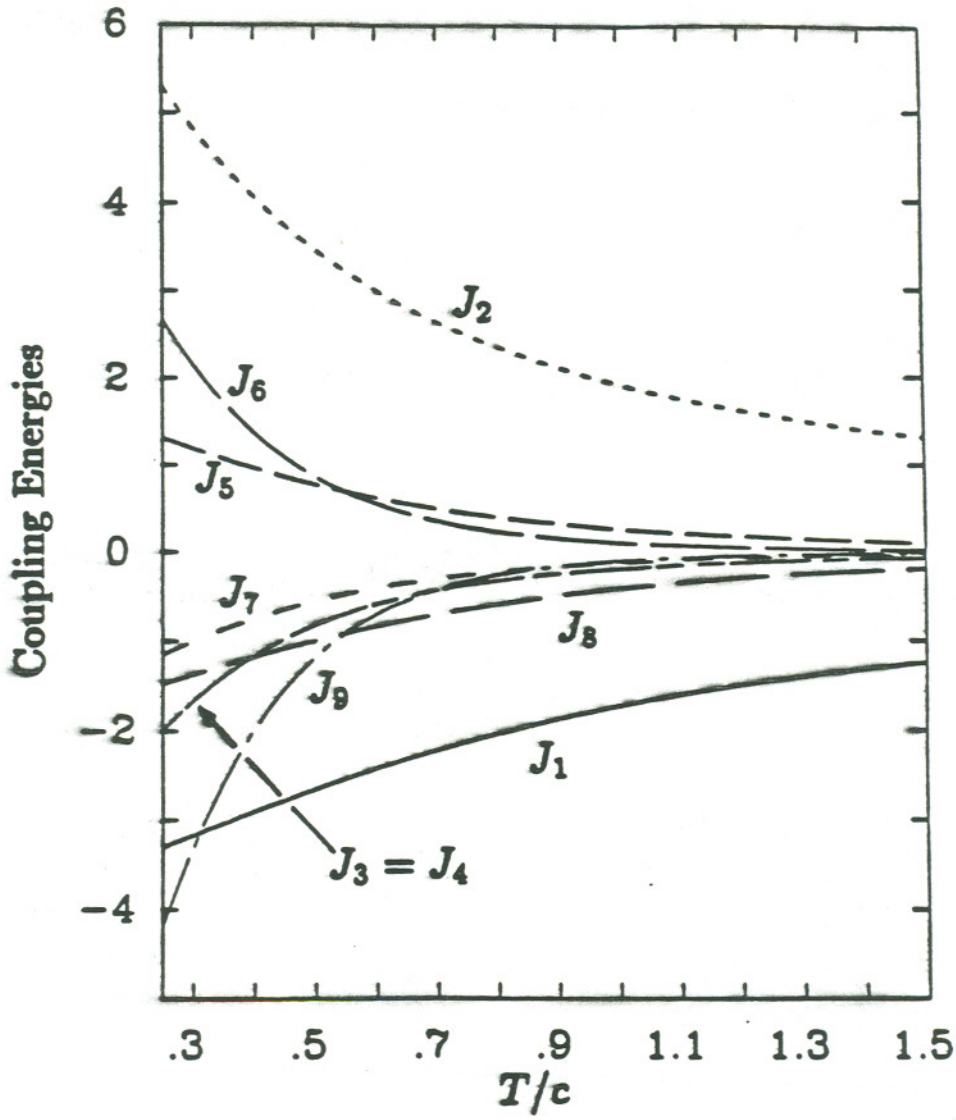
6
4
2
0
−2
−4
Coupling Energies
J_2
J_6
J_5
J_7
J_8
J_9
J_1
$J_3 = J_4$
.3
.5
.7
.9
1.1
1.3
1.5
T/c